DR. BEAT FREY (Orcid ID : 0000-0002-6391-3574)

Article type : Primary Research Articles

High temperatures enhance the microbial genetic potential to recycle C and N from necromass in high-mountain soils

Johanna Donhauser[1*], Weihong Qi[2], Benoît Bergk-Pinto[3], Beat Frey[1*]

[1]Rhizosphere Processes Group, Swiss Federal Institute for Forest, Snow and Landscape Research WSL, Zürcherstrasse 111, 8903 Birmensdorf, Switzerland

[2]Functional Genomics Center Zurich, ETH Zurich/University of Zurich, Winterthurerstr. 190, 8057 Zurich, Switzerland

[3]Environmental Microbial Genomics, Laboratoire Ampère, École Centrale de Lyon, Université de Lyon, 36 Avenue Guy de Collongue, 69134 Ecully, France

Running Title: Microbial necromass recycling with warming

***correspondence to:** Johanna Donhauser (johanna.donhauser@wsl.ch, +41 (0) 44 739 2315), Beat Frey (beat.frey@wsl.ch, +41 (0) 44 739 2541, ORCID iD: 0000-0002-6391-3574)

This article has been accepted for publication and undergone full peer review but has not been through the copyediting, typesetting, pagination and proofreading process, which may lead to differences between this version and the Version of Record. Please cite this article as doi: 10.1111/GCB.15492

Keywords: Climate change, high-mountain soil, C and N-cycling, metagenomes, bacterial growth, necromass, stress response

Abstract

Climate change is strongly affecting high-mountain soils and warming in particular is associated with pronounced changes in microbe-mediated C and N cycling, affecting plant-soil interactions and greenhouse gas balances and therefore feedbacks to global warming. We used shotgun metagenomics to assess changes in microbial community structures, as well as changes in microbial C- and N-cycling potential and stress response genes and we linked this data with changes in soil C and N pools and temperature-dependent measurements of bacterial growth rates. We did so by incubating high-elevation soil from the Swiss Alps at 4°C, 15°C, 25°C or 35°C for one month. We found no shift with increasing temperature in the C-substrate-degrader community towards taxa more capable of degrading recalcitrant organic matter. Conversely, at 35°C, we found an increase in genes associated with the degradation and modification of microbial cell walls, together with high bacterial growth rates. Together, these findings suggest that the rapidly growing high-temperature community is fueled by necromass from heat-sensitive taxa. This interpretation was further supported by a shift in the microbial N-cycling potential towards N mineralization and assimilation under higher temperatures, along with reduced potential for conversions among inorganic N forms. Microbial stress-response genes reacted inconsistently to increasing temperature, suggesting that the high-temperature community was not severely stressed by these conditions. Rather, soil microbes were able to acclimate by changing the thermal properties of membranes and cell walls as indicated by an increase in genes involved in membrane and cell wall modifications as well as a shift in the optimum temperature for bacterial growth towards the treatment temperature. Overall, our results suggest that high temperatures, as they may occur with heat waves under global warming, promote a highly active microbial community capable of rapid mineralization of microbial necromass, which may transiently amplify warming effects.

1. Introduction

High-mountain environments are currently warming rapidly. Temperatures are expected to increase by 2-6 °C by 2085 compared with values in 1981-2010 (CH2018, 2018; Gobiet et al., 2014). While warming-induced vegetation shifts in mountain ecosystems are relatively well understood (e.g. Steinbauer et al., 2018), belowground warming responses are still a "black box", despite their importance regarding global greenhouse gas budgets and plant-soil interactions (reviewed in Hagedorn et al., 2019). Microorganisms are key players mediating soil biogeochemical processes in high-elevation environments (Adamczyk et al., 2019; Donhauser & Frey, 2018; Rime et al., 2016). However, warming-induced changes in microbial community dynamics and associated alterations in biogeochemical cycles in these ecosystems remain poorly understood.

Higher temperatures are expected to enhance microbial activity and therefore mineralization of soil organic matter (SOM) associated with increasing CO_2 emissions and with depletion of carbon (C) and nutrients in the soil (Bradford et al., 2008; Dawes et al., 2017; Hagedorn et al., 2010; Melillo et al., 2002; Romero-Olivares et al., 2017). Various mechanisms that determine SOM mineralization or stabilization under warming have been proposed, including depletion of labile SOM and enrichment of recalcitrant plant-derived residues, recycling or stabilization of microbial necromass (Lehmann & Kleber, 2015; Mooshammer et al., 2014a). Regardless of the conceptual mechanism behind these SOM processes, soil scientists more and more appreciate the importance of different functional guilds in the microbial community driving C dynamics and increasingly include them in biogeochemical models (e.g. Huang et al., 2018; Kaiser et al., 2014). However, the existence of such functional guilds and their dynamics in response to increasing temperature have rarely been shown empirically in high-mountain soils.

To date warming responses of mountain soil microbial communities and associated changes in C and N resources have been assessed mostly with regard to taxonomic composition (Donhauser et al., 2020; Y. Li et al., 2016; Lulakova et al., 2019; Rui et al., 2015; Wu et al., 2015; Yu et al., 2019; Zhang et al., 2015; Zumsteg et al., 2013), where it remains challenging to infer alterations in microbial functional traits. Moreover, in marker gene sequencing studies, mostly bacteria have been investigated. In contrast, few studies have targeted eukaryotic microbial communities (Kerfahi et al., 2016; Nielsen et al., 2014) or microbial community dynamics across kingdoms, which can be indicative of symbiotic, parasitic or predator prey relationships. Such dynamics may enhance the turnover of microbial biomass and accelerate C and N cycling, owing to the release of labile C and N to the soil when microbial cells become lysed by e.g. parasites (Bardgett & Chan, 1999; Blagodatskaya et al., 2014; Clarholm, 1985; Kuzyakov & Mason-Jones, 2018), but remain poorly understood.

Laboratory warming studies using amplicon sequencing have revealed several taxa that consistently become more abundant at high temperatures, such as *Burkholderia-Paraburkholderia*, *Phenylobacterium* and *Pseudolabrys* (Donhauser et al., 2020; Jurburg et al., 2017a; Jurburg et al., 2017b; Wu et al., 2015) as well as taxa that typically become less abundant, such as *Mucilaginibacter* and *Cytophaga* (Donhauser et al., 2020; Lulakova et al., 2019). Although some of their functional capabilities are known (e.g. lignin degradation for *Burkholderia* (Tao et al., 2020) and cellulose and chitin degradation for *Mucilaginibacter* and *Cytophaga* (Štursová et al., 2012), it remains challenging to infer changes in functional traits among the microbial community from taxonomic studies and direct characterizations of the microbial functional potential in high-mountain ecosystems remain scarce. In high mountain ecosystems, a few studies have addressed specific functional guilds such as ammonia oxidizers (Yuan et al., 2015) and autotrophs (Guo et al., 2015) or used microarrays to investigate the microbial metabolic potential (Yang et al., 2014; Yue et al., 2015; Zhang et al., 2013). For instance, Yue et al. (2015) explained stable C and N stocks upon warming on the Tibetan plateau by increased inputs of labile organic matter (OM) from plants that suppressed microbial degraders of recalcitrant SOM, as inferred from a decrease in genes involved in this process using the microarray GeoChip. Similar feedback mechanisms, which compensated initial increases in microbial respiration, have been invoked in temperate ecosystems using shotgun metagenomics (Luo et al., 2014; Zhou et al., 2012). In high mountain-ecosystems, however, such a probe-independent investigation of the microbial functional potential in response to warming remains lacking.

With global warming, not only average temperatures are predicted to increase (leading to more energy available for microbial activity), but also maximum temperatures and the occurrence of temperature extremes are expected to rise considerably (CH2018, 2018; Gobiet et al., 2014). Microbial activity at the community level increases with temperature in a predictable manner up to T_{opt} (temperature where maximum activity occurs [Barcenas-Moreno et al., 2009; Rinnan et al., 2009; J. Rousk et al., 2012]). Temperatures above T_{opt}, however, rapidly lead to decreasing enzyme activity and cell damage and therefore exert a strong selective pressure on microbial communities (Barcenas-Moreno et al., 2009; van Gestel et al., 2013). Above-optimum temperatures have been shown to induce a shift in the peak of microbial growth towards higher temperatures (Barcenas-Moreno et al., 2009; Birgander et al., 2013). Donhauser et al. (2020) have shown that these shifts in growth rates coincided with strongly decreasing alpha-diversity and a pronounced shift in bacterial community structures towards dominance of a few heat-resistant genera. However, it has not been shown to date how these taxa accomplish resistance against heat-stress and which functional properties lead to their dominance at high temperature.

Moreover, high temperature and other stressful cues can induce lysis of sensitive taxa and thus provide

labile C and nutrients to survivors (Mooshammer et al., 2017). Therefore, high temperatures may additionally induce responses in C and N dynamics that are not predictable from the kinetic properties of microbial activity and substrate depletion upon increased activity alone. Hence, degraders of recalcitrant C might be suppressed transiently owing to nutrient pulses from microbial necromass (Donhauser et al., 2020). On the other hand, input of labile necromass C and N may induce priming and thus increase SOM mineralization and CO_2 emissions, depending on which nutrient is limiting (Cui et al., 2020; Mooshammer et al., 2014b; Rousk et al., 2016). The outcome of C- and N-cycling processes under high temperature critically depends on competitive dynamics among different functional guilds in the microbial community, but an in-depth understanding of changes in the microbial C- and N-cycling potential across large temperature ranges in alpine soils is lacking.

To address these gaps, in this study, we incubated a high-mountain soil from the European Alps (3100 m a.s.l.) at 4 (control), 15, 25 and 35 °C for one month. We determined bacterial temperature adaptation using ^{3}H-leucine incorporation and used shotgun metagenomics coupled with the characterization of changes in soil C and N pools to assess changes in the microbial functional potential with warming. Specifically, we were interested in temperature related shifts in

i) Taxonomic composition of bacteria as well as fungi and other microeukaryotes
ii) Functional genes that might confer survival at high temperature related to stress response and modification of thermal properties of biomolecules. Owing to the high selection pressure through thermal damage, we expected an increase in these genes at high temperature.
iii) C-cycling genes. As we expected rapid utilization of labile C sources owing to higher growth rates, we predicted an increase in genes involved in the degradation of recalcitrant SOM with increasing temperature.
iv) N-cycling genes. Owing to high metabolic demands associated with high microbial activity, we expected an increase in the microbial N assimilation potential at high temperature.

2. Materials and Methods

2.1. Site description and sampling

The mountain summit Piz Plazèr, where we sampled on the north slope, is located in the Eastern Swiss Alps (N46 ° 42.525’ E10 ° 23.307’) at 3094 m a.s.l. on siliceous bedrock. At this elevation vegetation is scarce (< 50% cover) and the north slope is dominated by mosses and lichens. In August 2016, with a shovel, we took five subsamples within a 5 m radius, which were subsequently pooled. We sampled from 2 - 20 cm depth (approx. 10l per subsample), removing plant above-ground parts and large roots by hand. Soil temperature at 5 cm depth was recorded from August 2016 to August 2018. The mean

soil temperature ranged from -16.17 to 19.19 °C throughout the year with a mean of -1.7 °C. The mean growing season (June - September 2017) soil temperature was 5.71 °C. The soil is poorly developed with a high sand fraction (89.8%) and a low water holding capacity (0.31 ml/g dry soil). The pH of the soil was 4.15. The soil was sieved at 4 mm mesh size and stored at 4 °C until the beginning of the experiment in March 2017.

2.2. Incubation experiment

After adjusting soil water content to 60% of the waterholding capacity with sterilized water, 20 g dry soil equivalent was filled into sterilized 100 ml Erlenmeyer flasks in triplicates per incubation temperature treatment. The experiment was set up at 4 °C. A 20 g aliquot was frozen at -20 °C as time 0 (T0) control. We sealed the flasks with autoclaved cellulose plugs and incubated the soils at 4, 15, 25 and 35 °C for 28 days. At the start of the incubation, we increased the temperature by 1.5 °C per 30 min until the target temperature was reached. The 4 °C samples represent the control at storage temperature. Water loss was compensated gravimetrically. This was done daily for the 25 and 35 °C treatments, every two days for the 15 °C treatment and weekly for 4 °C treatment. After the incubation period, we immediately froze the soils at -20 °C.

2.3. Chemical soil properties

Approximately 1.5 g soil from each of the incubated samples was dried at 65 °C for three days to determine its gravimetric water content. Subsequently the soil was ground with a mortar, 40 mg of soil from each sample were weighed into a tin cap and total carbon (TC) and total nitrogen (TN) contents were measured with a CHN analyzer (Shimadzu, Tokyo, Japan). In addition, 4 g fresh soil from each sample was extracted in 1M KCl (1:5 m/w) in an overhead shaker at room temperature for 1.5 h and filtered through paper filters (0790 1/2 Whatman paper filter, Whatman Inc., CA, USA). Dissolved organic carbon (DOC) and nitrogen (DON) concentration were determined from the extract using a TOC-V analyzer (Sakalar Analytical B.V, Breda, Netherlands). Ammonium (NH_4^+) was measured photometrically with a FIAS 300 (Perkin-Elmer, MA, USA). Nitrate (NO_3^-) concentration was determined using the UV-absorption method by Norman & Stucki (1981) but with $CuSO_4$-coated zinc granules as a reducing agent (Schleppi et al., 2012).

2.4. Temperature dependent measurement of ^{3}H-leucine incorporation

To determine changes in bacterial growth rates and temperature adaptation in response to warming, we measured ^{3}H-leucine incorporation at seven different temperatures as described previously (Donhauser et al., 2020). Briefly, immediately upon harvesting the experiment, we prepared a bacterial suspension in

water from 5 g from each of the incubated samples in 20 ml sterilized, deionized water. ^{3}H-leucine (37MBq ml^{-1} and 5.74 TBq mmol^{-1}; Perkin Elmer, USA) mixed with unlabelled leucine resulting in a final concentration of 275 nM was then added to 1.5 ml aliquots from the bacterial suspension from each sample. To measure the temperature dependence of leucine incorporation, aliquots were incubated at 4, 12, 18, 25, 30, 35 or 40 °C for samples that had been incubated at temperatures up to 25 °C and additionally at 45 °C for samples that had been incubated at 35 °C (henceforth, we refer to these temperatures as measurement temperatures). ^{3}H-leucine incorporation was terminated by adding trichloroacetic acid, and ^{3}H-activity of incorporated leucine was determined by liquid scintillation counting and then calculated per h and g dry soil.

2.5. Calculation of temperature dependent properties of ^{3}H-leucine incorporation (T_{min}, T_{opt})

To describe the bacterial temperature adaptation, we calculated T_{min} (minimum temperature for growth) and T_{opt} (temperature where maximum growth occurs; Bååth, 2018; Rinnan et al., 2009). To this end, we used the Ratkowsky square root model to determine the temperature dependence of bacterial growth according to equation 1 (Ratkowsky et al., 1983).

$$\sqrt{Leu} = a(T - T_{min}) \times (1 - e^{b(T - T_{max})}) \qquad (1)$$

where Leu is the ^{3}H-leucine incorporation rate, T is the measurement temperature, a and b are slope parameters, T_{min} is the minimum temperature for growth and T_{max} is the maximum temperature for growth. Below the optimum temperature, the equation can be expressed as a simplified linear function:

$$\sqrt{Leu} = a(T - T_{min}) \qquad (2)$$

We used equation 2 to estimate a and T_{min} (x-axis intercept), which were then used as constants to fit the model over the entire temperature range (equation 1). T_{opt} was calculated as the temperature where the first derivative of equation 1 equals 0.

2.6. DNA extraction, PCR, amplicon and shotgun sequencing

We extracted total DNA with the DNeasy PowerSoil Kit (Qiagen, Hilden, Germany) according to the manufacturer's instructions. To compare the taxonomic composition of microbial communities in our soil obtained from shotgun data with the taxonomic composition obtained from amplicon sequencing as applied in many previous studies in high-mountain soils (e.g. Donhauser et al., 2020), we also conducted amplicon sequencing of the bacterial 16S ribosomal RNA (rRNA) gene. To this end, the V3 - V4 region of 16S rRNA gene was PCR amplified with the primer pair 341F and 806R and PCR conditions as described previously (Frey et al., 2016) with 10 ng template DNA. Triplicate PCR reactions were pooled and sent to the Génome Québec Innovation Centre at McGill University (Montréal, Canada) for paired-end (PE) sequencing (read length = 300 base pairs (bp) on the Illumina MiSeq v3 platform (Illumina Inc., San Diego,

CA, USA). Shotgun library preparation and PE sequencing were also performed at the Génome Québec Innovation Centre using the NEB Next ultra II DNA Prep Kit (Illumina Inc., San Diego, California, USA) on an Illumina HiSeq 4000 PE100 system (Illumina Inc., San Diego, California, USA) yielding PE reads of 2x100 bp. Raw sequences were deposited in the NCBI Sequence Read Archive under the accession number PRJNA611981 for amplicon sequencing data and PRJNA650496 for shotgun data.

2.7. Processing of the sequencing data

2.7.1 Processing of 16S rRNA amplicon data

16S rRNA amplicon sequences were quality controlled, clustered into operational taxonomic units (OTUs) and taxonomically assigned as described previously (Donhauser et al., 2020) using a customized pipeline based on UPARSE (Edgar, 2013). The pipeline is based on clustering sequences into OTUs at 97% identity. Taxonomic classification was achieved using a naïve Bayesian classifier (Wang et al., 2007) querying against the SILVA v128 database (Quast et al., 2013). For details on the processing of amplicon sequencing data the reader is referred to Donhauser et al. (2020).

2.7.2. Metagenome assembly and functional annotation

We used a customized pipeline to analyze shotgun metagenomic data including pre-processing of shotgun reads, assembly of reads into contigs as well as prediction, functional annotation and abundance quantification of protein-coding genes and phylogenetic assignment of contigs. In brief, we used Trimmomatic v0.36 (adaptor trimming, minimum tail quality = 20, average quality = 20, minimum read length = 40; Bolger et al., 2014) to trim and filter the raw reads (henceforth referred to as pre-processed reads). Subsequently, we used the *de novo* de Bruijn graph assembler MEGAHIT v1.1.3 (–k-min 27 –k-step 10; D. Li et al., 2015) to assemble pre-preprocessed read pairs and singleton reads into contigs (> 200 bp). We applied MetaGeneMark v3.38 to predict protein-coding sequences in the contigs. To address changes in specific microbial functions with warming, we annotated the predicted genes against different databases: We used the broad and general database EggNOG (Huerta-Cepas et al., 2016) for i) an explorative analysis of changes in microbial functional genes and ii) for assessing changes in genes related with microbial stress response. EggNOG annotations were conducted via the md5nr database (Wilke et al., 2012), enabling the use of assembled metagenomes (Anwar et al., 2019). To assess changes in C-cycling genes, we annotated the predicted genes against the "Carbohydrate-Active EnZymes database" (CAZy; Cantarel et al., 2008). CAZy is organized based on evolutionary relationships among genes and we manually assigned categories grouping CAZy families by the recalcitrance of the C-substrate they target as well as by categories related to remodeling or degradation of microbial cell walls and membranes, respectively. To assess changes in N-cycling genes we annotated the predicted genes against a curated

database specific for N-cycling genes (NCycDB; Tu et al., 2018). Annotation against each of these databases was done with SWORD v1.0.3 (Vaser et al., 2016) with parameters (-v 10-5) as in Anwar et al. (2019).

2.7.3. Abundance quantification of protein-coding genes

Pre-processed read pairs from each sample were mapped back on the assembled contigs with the BWA aligner v0.7.15 (bwa-mem) (H. Li, 2013). The function *featureCounts* from the package Subread v1.5.1 (-minOverlap 10, Q=10, -primary, Liao et al., 2014) was used to count the reads mapped within the predicted protein coding. For the subsequent analyses with each of the functional databases (eggNOG, CAZy and NcycDB), the subset of genes annotated with the respective database was included.

2.7.4. Extraction of ribosomal RNA genes and taxonomic annotation

To assess the taxonomic composition of the metagenomes, we used the *-ssu_finder* function from CheckM (Parks et al., 2015) to identify small subunit ribosomal RNA (SSU rRNA) sequences contained in the contigs (16S for prokaryotes and 18S for eukaryotes). These sequences were then taxonomically annotated using the SILVA/SINA online aligner v1.2.11 (Pruesse et al., 2012).

2.7.5. Taxonomic classification of functional genes annotated with md5nr and CAZy

To link changes in microbial functional genes with changes in the taxonomic composition, we assessed the taxonomic affiliation of the functional genes annotated with eggNOG or with CAZy, respectively. Moreover, we compared changes in the taxonomic composition obtained by different approaches (classification of functional genes annotated with eggNOG or CAZy, extraction of ribosomal RNA genes and 16S rRNA amplicon sequencing) with increasing temperature.

For the taxonomic classification of functional genes annotated with eggNOG via the md5nr database, we used the MG-RAST API (http://api.mg-rast.org/m5nr/md5) to retrieve entries containing the NCBI taxID from different databases for the md5 identifiers found in our dataset. In some cases, multiple taxIDs were retrieved for one md5 ID, but these differed only at the strain level. Since we were not interested in classification beyond the genus level, we only used the first taxID to create a taxonomy for each md5 ID. Subsequently, we used the *getTaxonomy* function from the package taxonomizr (Sherrill-Mix, 2019) in R (R Core Team, 2018) to retrieve the taxonomy for each taxID at the desired levels.

For the taxonomic classification of functional genes annotated with CAZy, we converted the Genbank accession number into the NCBI taxID with an sqlite database created from the file prot.accession2taxid

downloaded from https://ftp.ncbi.nih.gov/pub/taxonomy/accession2taxid/ in R. Subsequently, we used the *getTaxonomy* function from the R package taxonomizr (Sherrill-Mix, 2019) to retrieve the taxonomy for each taxID at the desired levels.

2.8. Statistical analyses

All statistical analyses were conducted using R and plots were created with the ggplot R package (Wickham, 2009). R code used for this manuscript is available in the Supplementary Material. For a detailed specification of the parameters in each analysis the reader is referred to the R code.

Differences in soil C and N pools and in bacterial growth properties of soils incubated at different temperatures were assessed by one-way analysis of variance (ANOVA) followed by a Tukey HSD test. A Shapiro-test and Bartlett-test were used to assess the residuals normal distribution and homoscedasticity, respectively, and the response variables were log-transformed to fulfill the assumptions of ANOVA, if necessary.

We calculated alpha-diversity indices based on gene abundance matrices rarefied to even sequencing depth using the phyloseq R package (McMurdie & Holmes, 2013). As for chemical and bacterial growth parameters, we used one-way ANOVA followed by a Tukey HSD test to test for significant differences in observed richness and Shannon diversity with incubation temperature. To investigate differences in functional gene and community structures, we applied principal coordinate analysis (PCoA) based on Bray-Curtis differences of relative abundances (calculated from raw data). Permutational multivariate analysis of variance (PERMANOVA) was used to assess statistical significance. If significant differences were found for the full dataset, we subsequently removed the highest temperature and repeated the PERMANOVA for the subset, to evaluate if lower temperatures cause a significant shift in functional gene and community structures. To assess the relationship between chemical soil properties and bacterial growth parameters with functional gene and community structures, we regressed this data against the PCoA ordination scores using the *envfit* function in the vegan package (Oksanen et al., 2013) in R.

In order to assess changes in functional genes with increasing temperature we calculated $\log_2$-fold changes (LFC) at each temperature relative to the 4 °C control using DESeq2 (Love et al., 2014) with the apeglm shrinkage algorithm (Zhu et al., 2019). For each of the functional databases (eggNOG, CAZy and NcycDB, analyses were conducted separately and counts for genes annotated with the respective database were included in each analysis.

3. Results

3.1. Soil C and N pools and temperature dependence of bacterial growth

First, we assessed changes in different soil C and N pools with increasing temperature. Total carbon (TC) and total nitrogen (TN) ranged from 0.38% to 0.47% and from 0.039% to 0.046%, respectively, and did not change significantly with increasing incubation temperature (Table 1). However, the C:N ratio, ranging from 9.9 to 10.59 tended to be higher at 35 °C, but only the difference compared with 4 °C was significant. Dissolved organic carbon (DOC) was between 0.11 and 0.128 µg/g and did not change significantly with incubation temperature, while dissolved organic nitrogen (DON) was between 0.02 and 0.31 µg/g and was higher at 15 and 35 °C than at the other temperatures. The DOC:DON ratio was between 3.73 and 5.88 and decreased significantly at higher temperatures compared with 4 °C, especially at 15 and 35 °C. Ammonium (NH_4^+) was between 0.076 and 19.9 µg/g and was highest at 35 °C followed by 15 °C, while no significant differences were observed among the other temperatures. Nitrate (NO_3^-), ranging from 59.2 to 100.7 µg/g, was slightly higher at 15 °C than at 4 °C and significantly higher at 25 °C, while the concentration at 35 °C was equal to that at 4 °C.

Next, we investigated changes in bacterial growth rates as well as temperature adaptation with incubation temperature. ^{3}H-leucine incorporation, which we used as a proxy for bacterial growth, measured at 4 °C ranged from 181 to 990 $DPMg^{-1}h^{-1}$ and exhibited only marginal changes with incubation temperature, with higher values in the 35 °C samples (incubation temperature). Conversely, ^{3}H-leucine incorporation measured at 35 °C (ranging from 836 to 33636 $DPMg^{-1}h^{-1}$) was clearly higher in the 35 °C samples (incubation temperature) than in those from lower incubation temperatures (Table 1). T_{min} was between -7.97 and +0.785 °C and was higher at 35 °C compared with values for lower incubation temperatures (Table 1). Due to a high standard deviation, however, it was not significantly different compared to 15 °C incubation temperature. T_{opt} (the temperature where maximum bacterial growth occurred) ranged from 28.13 to 35.32 °C. It was slightly higher at 25 °C incubation temperature than at 4 or 15 °C and it showed an even more pronounced increase at 35 °C incubation temperature (Table 1). Collectively, these results indicate that, in response to the 35 °C incubation temperature treatment, the bacterial community transformed into one that performed better at higher temperature and generally grew more rapidly, while no changes (15 °C) or only slight changes (25 °C) occurred at lower incubation temperatures.

3.2. Overall metagenome sequencing results

After quality filtering, we obtained 640 495 401 metagenomic reads (42 699 693 ± 4 535 241 per sample). Table S1 gives an overview of the statistics for the processing of the metagenome data.

We were able to assemble 64.6% of the reads, resulting in 642 701 contigs > 1000 bp with an N50 value of 1608. The longest contig was 1 395 383 bp. In total 6 319 597 predicted genes were found among the contigs, of which we could annotate 8 388 with the general eggNOG database, 63 166 with the C-cycling gene database CAZy and 9 345 with the N-cycling gene database NCycDB. The number of reads mapping within genes annotated with each of the databases was 220 999 ± 129 831 per sample for eggNOG, 806 705 ± 260 417 for CAZy and 108 402 ± 39 398 for NCycDB. This corresponded 0.91, 3.2 and 0.45% of the reads mapped to predicted genes, respectively (Fig. S1). For each of the three functional databases the percentage of annotated reads remained constant up to 25 °C, but was slightly higher at 35 °C. 132 865 ± 53 276 reads per sample (0.55% of the total reads) were identified as ribosomal RNA using SINA.

3.3. Alpha-diversity

To assess if the functional and taxonomic diversity changed with incubation temperature, we calculated alpha-diversity indices (observed richness and Shannon diversity) of functional genes annotated with the each functional database (eggNOG, CAZy and NCycDB), as well as diversity of ribosomal genes (16S and 18S rRNA genes) extracted from the metagenomes in response to temperature. Observed richness did not change up to 25 °C, but was significantly reduced by about one fourth at 35 °C for functional genes annotated with eggNOG, CAZy and NCycDB, respectively, as well as ribosomal genes (Fig. 1). Shannon diversity for the three functional databases showed a similar pattern, however, for the ribosomal genes Shannon diversity was significantly reduced at 15 °C while no significant difference was observed at 35 °C (Fig. S2).

3.4. Shifts in functional gene structure and linkages with chemical soil parameters and bacterial growth parameters

To assess if overall functional gene structures and taxonomic composition changed with increasing incubation temperature, we conducted a principal coordinate analysis (PCoA). For the functional genes (eggNOG, C- and N-cycling genes) we found a gradual shift of structures with increasing temperature with a very pronounced difference at 35 °C. Permutational multivariate analysis of variance (PERMANOVA) showed significant results for all functional databases for the full dataset, with 35 °C samples removed, and with 25 and 35 °C samples removed (Table 2). Similarly, for the ribosomal genes the 35 °C samples were most different. In contrast to the functional databases, however, the 15 °C samples shifted more strongly than the 25 °C samples and also the direction of the shift was different compared with that observed for the 25 and 35 °C samples (Fig. 2). To assess the relationship between environmental variables and functional gene and community structures, we regressed the soil chemical and bacterial growth parameters against the PCoA ordination scores. We obtained significant relationships for T_{opt}, growth rates at 35°C, T_{min} and NH_4^+, which correlated positively with the shifts at 35 °C, for all functional databases and for the ribosomal

genes. For the ribosomal genes, NH_4^+ concentrations were additionally related to the shifts in community structures at 15 °C. Moreover, for the ribosomal genes DON showed a significant association that seemed mostly associated with changes in community structures at 15 °C. Further, for the ribosomal genes the C:N ratio showed a significant positive association with the 35 °C community structures, while the DOC:DON ratio was strongly negatively correlated with the 15 and 35 °C (Fig. 2).

3.5. Taxonomic composition

Next, we assessed changes in the taxonomic composition of the metagenomes with warming based on the functional genes annotated with eggNOG and CAZy to link changes in functional genes with the taxonomic affiliation of the genes. Moreover, we used the ribosomal genes extracted from the metagenomes to assess changes in the taxonomic composition including bacteria, archaea as well as fungi and other microeukaryotes. In addition, we compared this data with the taxonomic composition derived from 16S rRNA amplicon sequencing to evaluate to what extent taxonomic analyses based on metagenomes match those based on amplicon data. For the metagenome data, for all three databases approx. 90% of the reads were affiliated with bacteria (Figs. 3, S3).

For eggNOG, we found a pronounced increase in Proteobacteria at 35 °C and a decrease in all other phyla (Fig. 3). The most strongly decreasing phyla were Bacteroidetes, Cyanobacteria, Gemmatinomadetes and Verrucomicrobia. The fraction of Proteobacteria found with eggNOG was much higher than in the other databases at all temperatures.

For CAZy, similarly to eggNOG, we found an increase in Proteobacteria at 35 °C, while Bacteroidetes, Verrucomicrobia and Gemmatinomadetes decreased (Fig. 3). In contrast to the other databases, we found a significant proportion of Ascomycota and Streptophyta and moreover the fraction of Actinobacteria was significantly higher in CAZy, especially compared with eggNOG and the 16S rRNA amplicon data.

In contrast to the functional databases, for the ribosomal genes extracted from the metagenomes, we found a high abundance of Patescibacteria (approx. 25 %) at all temperatures except 35 °C (Fig. 3). Also for the 16S rRNA amplicon data, the abundance of Patescibacteria (designated as Saccharibacteria and Parcubacteria due to annotation with a different version of the SILVA database) was much lower than in the ribosomal genes extracted from the metagenomes. In addition, among the metagenome extracted rRNA genes, we found a high proportion of Dependentiae (also known as TM6) at 15 °C. At this temperature, we also observed an increase in Tubulinea (Amoebozoa), Cercozoa and Imbricatea (both Rhizaria) as well as unclassified Obazoa (Figs. 3, S3). Further, the ribosomal genes encompassed a considerable number of Mucoromycota as well as the bacterial candidate phylum WPS-2, which were not recovered with the

functional databases. Overall, we observed a decrease in the proportion of non-bacterial as well as unclassified sequences at 35 °C (Figs. 3, S3). Interestingly, Verrucomicrobia increased at 35 °C for the ribosomal genes from the metagenomes, while this phylum decreased for the functional databases and 16S rRNA amplicon data. Moreover, we found a slight increase in Crenarchaeota at 35 °C for the ribosomal genes extracted from the metagenomes.

The phyla Chloroflexi and Planctomycetes were overrepresented in the amplicon sequencing data compared with in the metagenomes. The phylum Cyanobacteria was represented by up to 8.3% proportion of reads within eggNOG and CAZy, while it was represented by less than 1% among ribosomal genes from metagenomes or amplicon sequencing.

3.6. Overall changes in functional genes and changes in stress-related genes with increasing temperature assessed with eggNOG

We used eggNOG to exploratively assess overall changes in functional genes and changes in stress-related genes in response to incubation temperature. Among the genes annotated with eggNOG, the most abundant level3 (broad categorization of all functions) categories were “energy production and conversion” (10.7%), “replication, recombination and repair (9.7%) and “amino acid transport and metabolism” (8.0%). None of the categories dominated the dataset and changes and abundances at different temperatures were mostly similar (Fig. S4).

In order to investigate changes in the abundance of functional genes with warming, we calculated $\log_2$-fold changes (LFC) at each incubation temperature relative to 4 °C for the genes annotated with eggNOG (8 388 genes in total). For $p_{adj} < 0.01$, at 15 °C we found 111 increased and 32 decreased genes. At 25 °C and 35 °C, 213 and 1 459 genes were overrepresented, and 232 and 2 690 genes were underrepresented, respectively. The full list of significant LFCs at 15 °C, 25 °C and 35 °C and descriptions of the functions are given in Table S2.

Aggregating over level3 functional categories, we found no significant LFC at 15 °C or 25 °C. At 35 °C, we found seven increased categories, among which ”cell wall/membrane/envelope biogenesis”, ”signal transduction mechanisms”, ”cell cycle control”, ”cell division” and ”chromosome partitioning” showed the greatest change. Conversely, seven categories diminished, with ”carbohydrate transport”, ”metabolism” and ”unknown function” showing the greatest change (Fig. 4).

Considering the 75 most abundant functions, most showed a positive LFC at all three temperatures

compared with 4 °C, most notably at 35 °C (Fig. 5, Table S3 lists descriptions of the functions in Fig. 5). At this temperature, however, the direction and magnitude of LFCs was highly variable for different genes with the same function.

At 15 °C, we observed a consistent increase in COGs within the category "translation, ribosomal structure and biogenesis" (COGs 0252, 0072 and 0441), the category "energy production in conversion" (COGs 3202 and 1034) as well as within the category "carbohydrate transport and metabolism" (COGs 0738, 3345, 2160, 0574 and NOG137180; Fig. 5).

At 25 °C, most decreased functions were found compared with the other temperatures. Within the category "posttranslational modification, protein turnover, chaperones", which contains many functions related to the thermal stress response, we found one decreased COG (COG0616, protease) at 25 °C as well as two increased COGs (the protease COG0465 and the chaperonin COG0459), which were also found at 35 °C with an even stronger increase. At 25 °C, strongly changing genes were widespread across taxonomy: functional genes were affiliated with many different genera within Proteobacteria (e.g *Phenylobacterium*, *Parvibaculum* and *Paraburkholderia*), Acidobacteria (e.g. *Candidatus Coribacter*) and Firmicutes (e.g. *Carboxydothermus*), while many decreasing genes were affiliated with the phylum Bacteroidetes, in particular the genera *Chitinophaga* and *Pedobacter* (Fig. S5).

Compared with at 25 °C, at 35 °C, functional genes were more narrowly distributed across taxonomy: most of the strongly increased genes belonged to Proteobacteria, namely the genera *Phenylobacterium*, *Caulobacter*, *Paraburkholderia*, *Burkholderia*, *Pseudomonas*, *Rhodopseudomonas* and *Parvibaculum* (Fig. S5). As we were particularly interested in stress responses, we assessed in more detail LFCs within the category "Posttranslational modification, protein turnover, chaperones" (Fig. S6), which contains proteases and chaperones playing an important role in refolding and degradation of heat damaged proteins (Ron, 2013). In addition to COG0465 and COG0459 mentioned above, further proteases and chaperones known to be involved in heat shock response were overrepresented at 35 °C. Among these were, for instance, heat-shock related COG0326 (HSP90 family chaperone) and COG0466 (Lon-protease). However, we also found six proteases and chaperones that decreased at 35 °C. These were, however, mostly represented by only one significantly changing gene (Fig. S6).

3.7. Changes in C-cycling genes with increasing temperature

Next, we assessed the C-utilization potential of the microbial community to evaluate if changes occurred because of altered substrate quantity and quality owing to increased microbial activity at elevated temperature. To this end, we annotated the metagenomes with the CAZy database. Overall, among the

genes annotated with CAZy, the most abundant enzyme classes at all temperatures were glycoside hydrolases (GH) and glycosyltransferases (GT), while polysaccharide lyases (PL) and auxiliary activities (AA) had the lowest abundance (Fig. S7 A). In total we found 375 different CAZy families in the sampled high-mountain soil (199 GHs, 58 GTs, 40 PLs, 17 AAs, 15 carbohydrate esterases (CE) and 47 carbohydrate binding modules (CBM). At the family level, GTs were especially abundant at all temperatures with GT2 (cellulose/chitin synthase and other functions) and GT4 (sucrose synthase and other functions) being the most abundant (Fig. S7 B).

As for overall changes in functional genes, to assess changes in the abundance of C cycling genes, we calculated $\log_2$-fold changes between the respective treatment temperature and 4 °C. Among the genes classified with the CAZy database (63 166 in total), for $p_{adj} < 0.01$, 474 genes increased at 15 °C and 48 decreased. At 25 °C 479 genes were elevated and 756 diminished, and at 35 °C 3392 increased and 12937 decreased. All significant LFCs and EC-numbers associated with each CAZy family are listed in Table S4. For most CAZy families genes within each family showed highly inconsistent patterns of change, with LFCs often ranging from -10 to +10, especially in increasing families. LFCs aggregated over families were considerably lower (approx. -3 to +4, Fig. 6). A more detailed description of the CAZy families displayed in Fig. 6 is provided in Table S5.

Aggregating over CAZy families, at 15 °C, the majority (10 out of 11) CAZy families increased, while at 25 and 35 °C, increasing and decreasing families were more evenly distributed. We did not find changes in C-utilization genes at any of the incubation temperatures (15, 25 and 35 °C) that pointed towards a consistent shift towards degraders of substrates of a particular recalcitrance (Fig. 6). This is to say CAZy families associated with substrates of opposing recalcitrance changed simultaneously (15 °C, 25 °C and 35 °C) or additionally, within the same category, shifts in different directions were observed (25 °C and 35 °C; Fig. 6).

Interestingly, however, many enzymes involved in degradation of murein (GH24, GH103, GH73, GH23, GH18 and CE4), as well as in modification of glycoproteins and other cell wall and membrane components (GT41, GT83, GT19, GT9, GT21, GT28, GH89, GH27, GH72, GH38, GH3, CE11 and CE9), increased significantly at 35 °C (Fig. 6). At this incubation temperature, we moreover detected a large number of strongly increased C-cycling genes among the proteobacterial genera *Phenylobacterium*, *Caulobacter*, *Ralstonia* and *Dyella* as well as among *Granullicella* (Acidobacteria). Genes belonging to *Phenylobacterium* and *Caulobacter* where particularly highly abundant across the dataset and thus likely drove the overall pattern when LFCs were aggregated over families (Fig. S8).

3.8. Changes in N-cycling genes with increasing temperature

As elevated temperatures potentially lead to accelerated N cycling, N limitation and changes in microbial N acquisition (Dawes et al., 2017; Rousk et al., 2016), we assessed changes in N-cycling genes using the NCyc database. Overall, the microbial community in the sampled high-mountain soil possessed high genetic versatility to carry out reactions in the N cycle, including the ability to fix N, to oxidize NH_4^+, as well as the potential for both dissimilatory and assimilatory NO_3^- reduction and denitrification.

To assess changes in N-cycling genes with increasing temperature, we calculated LFCs relative to 4 °C among the genes classified with NCycDB (9 345 in total). For $p_{adj} < 0.05$, at 15 °C, 52 genes significantly increased and 18 decreased. Aggregating over N-cycling genes, we detected no significant LFCs, however. At 25 °C, 133 genes significantly increased and 190 decreased. At 35 °C, 798 genes increased and 2492 decreased. A list of all significant LFCs is given in Table S6. The response among different variants of N cycling genes in the metagenomes was often highly inconsistent, especially for the category "organic degradation and synthesis" (Fig. 7).

At 25 °C, for the LFCs aggregated over genes represented in the database, three genes involved in "Organic degradation and synthesis" increased. Moreover, *narG* and *napA* (involved in denitrification and dissimilatory nitrate reduction) increased, while *narH* (belonging to the same process) and *pmoC* (involved in ammonia oxidation) decreased.

At 35 °C, all genes involved in "organic degradation and synthesis" as well as in "assimilatory nitrate reduction" increased. Conversely, genes involved in nitrification, nitrogen fixation, denitrification and anammox decreased. Likewise, most of the genes annotated with both denitrification and dissimilatory nitrate reduction decreased, with the exception of *narZ* and *napA*.

4. Discussion

4.1. Overall changes in functional and structural genes

In our warming experiment, the richness of functional and ribosomal genes slightly decreased at an incubation temperature of 25 °C and strongly decreased at 35 °C (Fig. 1). The same pattern has been observed previously based on 16S rRNA amplicon sequencing in the soil used in this study as well as in other mountain soils (Donhauser et al., 2020). Similarly, other authors reported strongly decreasing alpha-diversity at high temperatures and other stressors in amplicon (Lulakova et al., 2019; Wu et al., 2015) and metagenome sequencing studies (Santillan et al., 2019). Donhauser et al. (2020) recently found that the threshold where high temperature significantly diminishes diversity and strongly alters microbial

community structures coincides with the annual maximum temperature that soils experience naturally. In line with these observations, we found a gradual shift in functional gene structures with increasing temperature for the functional databases, which was small up to 25 °C and very pronounced at 35 °C, along with analogous shifts in bacterial growth parameters (growth rates at 35 °C, T_{min}, T_{opt}; Fig. 2, Table 1).

4.2. Taxonomic changes

In accordance with previous metagenomic studies, our dataset was strongly dominated by bacteria (Aalismail et al., 2019; Choi et al., 2017; Kerfahi et al., 2019). It has been recognized that eukaryotes may be underrepresented in metagenome datasets due to database and gene prediction biases (Del Campo et al., 2014; Jacquiod et al., 2016; Mathé et al., 2002). Interestingly, for the ribosomal genes extracted from the metagenomes, the community structures did not follow the gradual shift with increasing temperature observed for the functional databases and for 16S rRNA amplicons. Conversely, the shift at 15 °C was stronger than at 25 °C and the direction of shift was different compared with the pattern observed for samples at higher temperatures (25 and 35 °C; Fig. 2).

The shift in community structures at 15 °C in the metagenome extracted ribosomal genes was related to a pronounced increase in the candidate phylum Dependentiae (also known as TM6, Fig. 3). Dependentiae are characterized by small (1 - 1.5 Mb), streamlined genomes with reduced metabolic capabilities (McLean et al., 2013; Rinke et al., 2013; Yeoh et al., 2015). They are thought to be symbionts or parasites of microeukaryotes such as Amoeba and Ciliates (Delafont et al., 2015; McLean et al., 2013; Yeoh et al., 2015), which is supported in our study by their simultaneous increase in abundance at 15 °C together with Amoebozoa, Obazoa and Rhizaria (Fig. 3, Fig. S3). Parasitic interactions may accelerate the turnover of microbial biomass and contribute to the release of labile C and nutrients in the soil through lysis of host cells (Bardgett & Chan, 1999; Blagodatskaya et al., 2014). In accordance with this notion, together with the concurrent increase in Dependentiae and their eukaryotic hosts at 15 °C, we observed and increase in DON, NH_4^+ and in NO_3^-. Tracing isotopically labelled microorganisms into microbial DNA and soil C or N pools may contribute to substantiate the proposed interactions and the release of C and N from lysed cells in the future.

Interestingly, the uncultured candidate phylum Patescibacteria displayed a high abundance (approx. 30%) in the metagenome extracted ribosomal genes up to 25 °C, with a pronounced decrease at 35 °C. Patescibacteria showed a similar trend for the 16S rRNA amplicon data, but were represented in a much lower abundance, while they were entirely absent among the functional databases. A primer bias is a likely cause for the discrimination against Patescibacteria in amplicon sequencing data (Brown et al., 2015; Dudek et al., 2017; Eloe-Fadrosh et al., 2016; Klindworth et al., 2013), while the lack of matches in the

functional databases is likely explained by the fact that the latter are based on culturable taxa (Cantarel et al., 2008; Galperin et al., 2015; Huerta-Cepas et al., 2016; Pignatelli et al., 2008). Overall, our data highlights the potential of metagenomic analyses to overcome technical biases associated with amplicon sequencing and contribute to improved characterization of poorly described microbial taxa. Moreover, through the simultaneous analysis of different microbial kingdoms, we were able to demonstrate the co-occurrence of Dependentiae and their potential eukaryotic hosts.

4.3. Overall functional responses and changes in stress-related genes (eggNOG)

At 15 °C, we found no changes in stress-related genes. Conversely, we found a consistent increase in functions within the categories "translation, ribosomal structure and biogenesis", "energy production and conversion" and "carbohydrate transport and metabolism". This temperature alleviates thermal constraints to growth present at 4 °C, but is well below T_{opt} of bacterial growth and therefore does not impose thermal stress on the community. The increase in the abovementioned categories may indicate enhanced capacity to utilize C sources for growth and energy production. Contrary to this notion, bacterial growth rates were however not higher at 15 °C than at 4 °C. Many of the functions that increased at 15 °C are widespread across the taxonomy of microorganisms, or even housekeeping genes, such as the aminoacyl-tRNA transferases within "translation, ribosomal structure and biogenesis" (Chaliotis et al., 2017; Koonin & Aravind, 1998). The link between such common genes and microbial growth may be established more reliably at the gene expression level as e.g. in Coolen & Orsi (2015).

At 25 °C, we observed slight changes in some stress-related functions. (Fig. 5). This temperature corresponds approx. to T_{opt} of bacterial growth (Table 1), i.e. the temperature to which the majority of the community is presumably adapted (Donhauser et al., 2020). At 35 °C, which exceeds the natural temperature range of the sampled soil and induces a shift in T_{opt} of bacterial growth (Table 1; Donhauser et al., 2020), pronounced changes in several categories of eggNOG functions occurred (Figs. 5, S5). At this temperature, several proteases and chaperones increased, some of which are associated with microbial responses to thermal stress (e.g. the *lon* protease COG0465 and the chaperones COG0459 (*groEL*) and COG0326 (*hsp90* family). Proteases can degrade heat-damaged proteins while chaperones assure proper folding and protect proteins from irreversible aggregation (Hartman et al., 1993; Mendoza et al., 1996). The importance of chaperones under stressful conditions and environments has been reported previously in the context of an alpine soil aridity gradient (Song et al., 2019), aeolian dust samples (Aalismail et al., 2019) and desert environments (Le et al., 2016; Noronha et al., 2017). It should be noted, however, that the increase in functions related to heat stress response in our study was not consistent, as we also found proteases and chaperones that decreased at 35 °C.

In addition, we found an increase in the category ”signal transduction mechanisms”. This increment possibly represents the selection of organisms with efficient and tightly regulated responses to environmental stimuli thus enabling acclimation to pronounced changes in temperature. Lauro et al. (2009) highlighted that copiotrophic microbes typically display these properties and that components of signal transduction were overrepresented in copiotrophs compared to oligrophs in their study, where genomic features of copiotrophic and oligotrophic marine bacteria were compared. Therefore, our findings are in accordance with an increase in copiotrophs at high temperature in response to C and nutrient release from thermosensitive microbes (Donhauser et al., 2020; Mooshammer et al., 2017).

It is important to note that genes with the same function, and partly also those with similar functions within the same category, reacted inconsistently to higher temperatures (regarding both the direction and magnitude of change). One possible explanation is that the respective functions are not under selection. This is to say, the aggregate increase or decrease in some functions (i.e. when summing all genes within each function) is the byproduct of the selection of some organisms that increase in abundance owing to other properties. Accordingly, at 35 °C increasing genes belonged to a limited number of taxa, with a few highly abundant genera, such as *Phenylobacterium*, *Caulobacter* and *Paraburkholderia* represented in almost all increasing functions. *Phenylobacterium* and *Burkholderia-Paraburkholderia* have previously been found to respond positively to high temperatures in both alpine and temperate soils (Donhauser et al., 2020; Jurburg et al., 2017b; Nunes et al., 2018).

Generally, under stressful conditions, microbes face a trade-off in resource allocation to growth or survival (Aertsen & Michiels, 2004; Ferenci, 2016; Gudelj et al., 2010; Maharjan et al., 2013). For instance, in yeast the expression of stress response genes has been shown to be negatively correlated with growth rates (Brauer et al., 2008). Our interpretation of the patterns described above is, that 35 °C does not represent an extremely stressful environment for the genera that become highly abundant at high temperature. They may benefit from temperature acclimation mechanisms such as cell wall and membrane remodeling, promoting their dominance. However, we consider it unlikely that their heat resistance and expansion is the result of an acute, global stress response, as such a response would require too many resources to sustain the strong enrichment we observed.

4.4. Changes in the microbial C-cycling potential

Besides directly affecting the metabolism and survival of microorganisms, changes in temperature induce indirect effects, such as depletion of C and nutrients, as a consequence of an increased metabolic

rate at higher temperature (Bradford et al., 2008; Dawes et al., 2017; Hagedorn et al., 2010; Melillo et al., 2002; Romero-Olivares et al., 2017). Findings from these previous studies have suggested that elevated temperature leads to enrichment of recalcitrant SOM and an increase in taxa capable of degrading these substrates under warming has been supported by amplicon (DeAngelis et al., 2015) and metagenomic studies (Zhang et al., 2017). Other long-term studies have conversely reported a shift in microbial C-substrate degradation towards more labile substrates, which was attributed to increased plant inputs (Luo et al., 2014; Zhou et al., 2012). In our study, we found no detectable changes in TC or in DOC (representing a more readily available C pool, Table 1), which is in accordance with findings from an incubation study with similar duration (Ogwu et al., 2019). At 15 °C, the majority of differentially abundant CAZy families increased, pointing towards an increased C-cycling potential (Fig. 6). This notion, however, was contradicted by a constant number of all CAZymes as a fraction of predicted genes (Fig. S1), and was not reflected in changes in soil C pools. Among C-cycling genes, we did not observe a consistent increase or decrease in the abundance of degraders of particular C substrates (Fig. 6). On the contrary, we found either several categories along the labile-recalcitrant spectrum to increase (15 °C) or ambiguous shifts within the same category (25 and 35 °C). Thus, based on our metagenome data, we conclude that a shift in the SOM degrader community towards more recalcitrant substrates did not occur in our experiment, suggesting that soil microbes were not limited in labile C after the incubation period of one month. Our results are supported by findings from field studies, where changes in microbial community structures in response to altered substrate quantity and quality have been observed only after several years to decades (DeAngelis et al., 2015; Melillo et al., 2017; Rinnan et al., 2007; Romero-Olivares et al., 2017). However, direct characterization of temperature-induced changes in the quality of SOM is needed to corroborate these conclusions.

Further, we expected that high temperature leads to lysis of temperature-sensitive microbes, providing energy and nutrients to heat-resistant survivors and compensating increased use of labile C. In support of this notion, we found a strong increase in bacterial growth after incubation at 35 °C (Table 1, Donhauser et al., 2020). Moreover, we found many GHs involved in the degradation of bacterial cell walls enriched at 35 °C (Fig. 6). The recycling of cell wall components such as peptidoglycan from microbial necromass by microbes has been recognized as an important C and N source in soil (Basler et al., 2015; Guenet et al., 2011; Hu et al., 2017; Kindler et al., 2006). In addition, various studies have previously stressed the importance of C and nutrient release from vulnerable cells as energy and nutrient sources upon stressful stimuli like heat, radiation and freeze-thaw transitions (Mooshammer et al., 2017; Perez-Mon et al., 2020; Schostag, Anwar, et al., 2019; Schostag, Priemé, et al., 2019). The capability to decompose microbial cell walls might enable heat resistant microbes to capitalize on the death of heat-sensitive taxa under high

temperature and promote the dominance of the former.

In addition, we found an increase in GTs involved in murein synthesis at 35 °C (Fig. 6). Bacterial cell walls are subject to extensive turnover processes through the concerted action of peptidoglycan hydrolases and synthetases and bacteria have been shown to remodel their cell wall in response to changing environmental conditions (Bernal-Cabas et al., 2015; Cava & de Pedro, 2014; Horcajo et al., 2012). Thus, the enzymes involved in cell wall degradation and synthesis, which were overrepresented at 35 °C in this study, might contribute to maintaining cell wall homeostasis under high temperature regimes enabling acclimation. Similarly, enzymes involved in the degradation and synthesis of glycoproteins and lipopolysaccharides might contribute to changing the thermal properties of membranes and enable acclimation to different temperatures. Such protein and lipid modifying enzymes were found to increase at 35 °C in this study. Besides the CAZy families associated with cell wall and membrane processes, also with eggNOG, we found an increase at 35 °C in genes involved in outer membrane and cell wall biogenesis (COG0399 and COG2982) as well as in the entire category ”cell wall/membrane/envelope biogenesis” (Fig. 4) supporting the temperature induced changes in membrane and cell walls described above.

Similarly to the general functional annotation with eggNOG, genes within each CAZy family reacted very inconsistently, and highly increased genes were affiliated with a few abundant genera (*Phenylobacterium*, *Caulobacter*, *Ralstonia* and *Dyella*) that have previously been found to respond positively to high temperature (Donhauser et al., 2020; Jurburg et al., 2017a; Jurburg et al, 2017b) et. Similar to the eggNOG functions, this may indicate that some CAZy families are not selected for directly but change in abundance because of an enrichment or reduction of the organisms possessing them, owing to other properties.

4.5 Changes in the microbial N-cycling potential and linkages with C cycling

The studied soil was relatively low in SOM (TC ≈ 0.5%) and the DOC:DON ratio (considered most indicative of the C:N stoichiometry of microbe-available resources [Mooshammer et al., 2014a]) of 4 to 6 (Table 1) was significantly below the threshold C:N ratio of 21 where microbial communities can be considered C or N limited, respectively (Soong et al., 2020) at all temperatures. This indicates that the microbial communities in the sampled soil were primarily C limited. We hypothesize that the high N mineralization at 35 °C (inferred from increased NH_4^+ and DON concentrations, Table 1) was derived from lysis and microbial processing of heat-sensitive microorganisms. In support of this hypothesis, we observed an increase in several genes involved in N mineralization (e.g. *gdh* and *ureC*, Fig. 7*)* at 35 °C. At the same time many genes involved in N assimilation increased (*gdh, gs* and *glnA*, Fig. 7). Therefore, despite overall C limitation, the fast-growing taxa prevalent at 35 °C may have benefitted from a high N acquisition

potential, enabling rapid growth fueled from necromass N. In line with this view, fast-growing microorganisms have been proposed to have a relatively high N demand (Fierer et al., 2007; Mooshammer et al., 2014a). Wang et al. (2020) recently developed a ^{15}N-tracing model based on incubation of ^{15}N-labelled microbial necromass at different temperatures. With this approach, they were able to track necromass N into living biomass, inorganic N pools and mineral-associated necromass. After 21 days (most similar to the duration of our experiment), they recovered approx. 10% of the necromass ^{15}N in the living microbial biomass, while more than 50% was recovered as NH_4^+-N. Thus, similarly to in Wang et al. (2020), mineralization of necromass N may also explain the strong increase in NH_4^+ concentrations at 35 °C in this study. As microbial biomass is rich in N (Xu et al., 2013), and the fast-growing high-temperature community is assumed to have a high energy demand, recycling of microbial necromass is expected to exacerbate the C limitation in the studied soil, which is supported by the decreased DOC:DON ratio at 35 °C compared with 4 °C as well as by the strong increase in inorganic N at 35 °C (Table 1).

Overall, we found a shift in the microbial N-cycling potential towards N assimilation and mineralization of organic N and away from transformations of inorganic N forms (increase in all genes involved in "organic degradation and synthesis" and "assimilatory nitrate reduction", decrease in all other categories at 35 °C, Fig. 7). Notably, genes involved in NH_4^+ oxidation to NO_2^- and further oxidation to NO_3^- (*amoA* [ammonium monooxygenase], *hao* [hydroxylamine oxidoreductase], *nxrA* and *B* [nitrite oxidoreductase A and B] and genes potentially involved in NH_4^+ oxidation (*pmoA*, *B* and *C* [particulate methane monooxygenase]) decreased at high temperature (35 °C), despite high NH_4^+ concentrations. From 4 to 25 °C, we observed a stepwise increase in NO_3^- concentration and at 25 °C we observed the lowest NH_4^+ concentrations, suggesting increased conversion of NH_4^+ to NO_3^- (nitrification) with increasing temperature. At 35 °C, however, NO_3^- concentrations were not different from at 4 °C, suggesting that nitrification was suppressed, which is in line with the decrease in genes involved in this process. Since ammonia oxidizers were not deprived of NH_4^+, we speculate that their decrease was related to high-temperature sensitivity. Alternatively, since most *amoA* genes retrieved at all temperatures belonged to archaeal ammonia oxidizers that are adapted to low NH_4^+ concentrations (Hatzenpichler, 2012; He et al., 2012), the strongly increased NH_4^+ concentrations at 35 °C (approx. 15-fold increase compared to 4 °C) might have suppressed archaeal ammonia oxidizers.

At 15 °C we found a slight increase in NO_3^- and DON and a pronounced increase in NH_4^+ compared with at 4 °C (Table 1). These changes in N compounds were not linked with changes in functional genes, but were significantly correlated with the community structures from metagenome extracted ribosomal genes (Fig. 2). Therefore, we suggest that the N dynamics at 15 °C were linked with changes in the microbial community that were recovered only with the ribosomal genes and not with the functional

databases, such as the pronounced increase in Dependentiae together with their putative eukaryotic hosts. For instance, parasitic interactions might release N compounds to the soil, similarly to heat-induced lysis of microbial cells (Bardgett & Chan, 1999; Blagodatskaya et al., 2014). In support of this notion, we observed similar changes in N pools at 15 °C relative to 4 °C compared with the changes at 35 °C, which did not occur at 25 °C (e.g. increase in DON and NH_4^+ concentrations, Table1). Direct tracking of N compounds in the soil and microbial biomass would help to substantiate these proposed mechanisms.

4.6. Conclusion

Collectively, our metagenomic analysis of a high-mountain soil revealed important changes in the microbial functional potential in response to increasing temperature with regard to both C and N cycling. While the potential to degrade C sources of varying recalcitrance was not affected within the time scale of this study, changes in C-cycling genes suggested that microbial necromass from heat-sensitive taxa was an important source of C and nutrients fueling rapid growth of the high-temperature community at 35 °C. Similarly, changes in N pools and N-cycling genes suggested high N mineralization and N-assimilation potential, suggesting that the high temperature community benefitted from necromass N. Inconsistent responses in microbial stress genes together with high growth rates at high temperature indicate that the dominant taxa at this temperature were not severely stressed but adapted to these conditions. Recycling of microbial necromass has generally been recognized to play an important role in C dynamics and SOM formation (Cui et al., 2020; Lehmann & Kleber, 2015; Mooshammer et al., 2014b). Overall, our data indicates that recycling of microbial necromass plays a particularly critical role in shaping microbial community dynamics and thus C and N dynamics in high-mountain soils under high temperatures, as they may occur with heat waves under global warming. Under such conditions, necromass recycling may exacerbate C limitation in these low-biomass soils. Combining metagenomic approaches as used in this study with isotopic labelling studies as in e.g. Wang et al. (2020) could provide a powerful approach to couple SOM and necromass turnover processes with microbial community dynamics in response to warming in the future.

Acknowledgements

We thank the Environmental Microbial Genomics Group at ECL Lyon, especially Catherine Larose and Timothy Vogel for valuable discussions about this study. We thank the Central laboratory at the Swiss Federal Institute WSL for laboratory support. Moreover, we would like to thank Melissa Dawes for English corrections. We acknowledge the Genetic Diversity Center (GDC) at ETH Zurich for providing access to high-performance computing facilities. Further, we acknowledge the contribution of scientists at the McGill

University and Génome Québec Innovation Center, Montréal, Canada, for the paired-end Illumina MiSeq and HiSeq sequencing. This study was funded by the MicroArctic Innovative Training Network grant supported by the European Commissions's Marie Sklodowska Curie Actions program under project number 675546.

Author contributions: J.D. and B.F. conceived the ideas. J.D. performed laboratory work. J.D. and W.Q. analyzed the data. All authors prepared and approved the final version of the manuscript.

Conflict of interest: The authors declare no conflict of interest.

Data and materials availability: The data that supports the findings of this study are available at the NCBI Sequence Read Archive (https://www.ncbi.nlm.nih.gov/sra) under the accession numbers PRJNA611981 and PRJNA650496 (sequencing data) or from the corresponding author upon request (all other data).

6. References

Aalismail, N. A., Ngugi, D. K., Díaz-Rúa, R., Alam, I., Cusack, M., & Duarte, C. M. (2019). Functional metagenomic analysis of dust-associated microbiomes above the Red Sea. *Scientific Reports*, *9*(1), 1–12. https://doi.org/10.1038/s41598-019-50194-0

Adamczyk, M., Hagedorn, F., Wipf, S., Donhauser, J., Vittoz, P., Rixen, C., Frossard, A., Theurillat, J.-P., & Frey, B. (2019). The Soil Microbiome of GLORIA Mountain Summits in the Swiss Alps. *Frontiers in Microbiology*, *10*, 1080. https://doi.org/10.3389/fmicb.2019.01080

Aertsen, A., & Michiels, C. W. (2004). Stress and how bacteria cope with death and survival. *Critical Reviews in Microbiology*, *30*(4), 263–273. https://doi.org/10.1080/10408410490884757

Anwar, M. Z., Lanzen, A., Bang-Andreasen, T., & Jacobsen, C. S. (2019). To assemble or not to resemble-A validated Comparative Metatranscriptomics Workflow (CoMW). *GigaScience*, *8*(8), 1–10. https://doi.org/10.1093/gigascience/giz096

Bååth, E. (2018). Temperature sensitivity of soil microbial activity modeled by the square root equation as a unifying model to differentiate between direct temperature effects and microbial community adaptation. *Global Change Biology*, *24*(7), 2850–2861. https://doi.org/10.1111/gcb.14285

Barcenas-Moreno, G., Gomez-Brandon, M., Rousk, J., & Bååth, E. (2009). Adaptation of soil microbial communities to temperature: comparison of fungi and bacteria in a laboratory experiment. *Global Change Biology*, *15*(12), 2950–2957. https://doi.org/10.1111/j.1365-2486.2009.01882.x

Bardgett, R. D., & Chan, K. F. (1999). Experimental evidence that soil fauna enhance nutrient mineralization and plant nutrient uptake in montane grassland ecosystems. *Soil Biology and Biochemistry*, *31*(7), 1007–1014. https://doi.org/10.1016/S0038-0717(99)00014-0

Basler, A., Dippold, M., Helfrich, M., & Dyckmans, J. (2015). Microbial carbon recycling - An underestimated process controlling soil carbon dynamics - Part 1: A long-term laboratory incubation experiment. *Biogeosciences*, *12*(20), 5929–5940. https://doi.org/10.5194/bg-12-5929-2015

Bernal-Cabas, M., Ayala, J. A., & Raivio, T. L. (2015). The Cpx envelope stress response modifies peptidoglycan cross-linking via the L,D-transpeptidase LdtD and the novel protein YgaU. *Journal of Bacteriology*, *197*(3), 603–614. https://doi.org/10.1128/JB.02449-14

Birgander, J., Reischke, S., Jones, D. L., & Rousk, J. (2013). Temperature adaptation of bacterial growth and 14C-glucose mineralisation in a laboratory study. *Soil Biology & Biochemistry*, *65*, 294–303. https://doi.org/10.1016/j.soilbio.2013.06.006

Blagodatskaya, E., Khomyakov, N., Myachina, O., Bogomolova, I., Blagodatsky, S., & Kuzyakov, Y. (2014). Microbial interactions affect sources of priming induced by cellulose. *Soil Biology and Biochemistry*, *74*, 39–49. https://doi.org/10.1016/j.soilbio.2014.02.017

Bolger, A. M., Lohse, M., & Usadel, B. (2014). Trimmomatic: A flexible trimmer for Illumina sequence

data. *Bioinformatics*, *30*(15), 2114–2120. https://doi.org/10.1093/bioinformatics/btu170

Bradford, M. A., Davies, C. A., Frey, S. D., Maddox, T. R., Melillo, J. M., Mohan, J. E., Reynolds, J. F., Treseder, K. K., & Wallenstein, M. D. (2008). Thermal adaptation of soil microbial respiration to elevated temperature. *Ecology Letters*, *11*(12), 1316–1327. https://doi.org/10.1111/j.1461-0248.2008.01251.x

Brauer, M. J., Huttenhower, C., Airoldi, E. M., Rosenstein, R., Matese, J. C., Gresham, D., Boer, V. M., Troyanskaya, O. G., & Botstein, D. (2008). Coordination of growth rate, cell cycle, stress response, and metabolic activity in yeast. *Molecular Biology of the Cell*, *19*(1), 352–367. https://doi.org/10.1091/mbc.E07-08-0779

Brown, C. T., Hug, L. A., Thomas, B. C., Sharon, I., Castelle, C. J., Singh, A., Wilkins, M. J., Wrighton, K. C., Williams, K. H., & Banfield, J. F. (2015). Unusual biology across a group comprising more than 15% of domain Bacteria. *Nature*, *523*(7559), 208–211. https://doi.org/10.1038/nature14486

Cantarel, B. L. I., Coutinho, P. M., Rancurel, C., Bernard, T., Lombard, V., & Henrissat, B. (2008). The Carbohydrate-Active EnZymes database (CAZy): an expert resource for Glycogenomics. *Nucleic Acids Research*, *37*(suppl_1), D233–D238. https://doi.org/10.1093/nar/gkn663

Cava, F., & de Pedro, M. A. (2014). Peptidoglycan plasticity in bacteria: Emerging variability of the murein sacculus and their associated biological functions. *Current Opinion in Microbiology*, *18*(1), 46–53. https://doi.org/10.1016/j.mib.2014.01.004

CH2018. (2018). *CH2018 – Climate Scenarios for Switzerland, Technical Report*. National Centre for Climate Services.

Chaliotis, A., Vlastaridis, P., Mossialos, D., Ibba, M., Becker, H. D., Stathopoulos, C., & Amoutzias, G. D. (2017). The complex evolutionary history of aminoacyl-tRNA synthetases. *Nucleic Acids Research*, *45*(3), 1059–1068. https://doi.org/10.1093/nar/gkw1182

Choi, S., Song, H., Tripathi, B. M., Kerfahi, D., Kim, H., & Adams, J. M. (2017). Effect of experimental soil disturbance and recovery on structure and function of soil community: A metagenomic and metagenetic approach. *Scientific Reports*, *7*(1), 1–15. https://doi.org/10.1038/s41598-017-02262-6

Clarholm, M. (1985). Interactions of bacteria, protozoa and plants leading to mineralization of soil nitrogen. *Soil Biology and Biochemistry*, *17*(2), 181–187. https://doi.org/10.1016/0038-0717(85)90113-0

Coolen, M. J. L., & Orsi, W. D. (2015). The transcriptional response of microbial communities in thawing Alaskan permafrost soils. *Frontiers in Microbiology*, *6*(197). https://doi.org/10.3389/fmicb.2015.00197

Cui, J., Zhu, Z., Xu, X., Liu, S., Jones, D. L., Kuzyakov, Y., Shibistova, O., Wu, J., & Ge, T. (2020). Carbon and nitrogen recycling from microbial necromass to cope with C:N stoichiometric imbalance by priming. *Soil Biology and Biochemistry*, *142*(August 2019), 107720.

https://doi.org/10.1016/j.soilbio.2020.107720

Dawes, M. A., Schleppi, P., Hättenschwiler, S., Rixen, C., & Hagedorn, F. (2017). Soil warming opens the nitrogen cycle at the alpine treeline. *Global Change Biology*, *23*(1), 421–434. https://doi.org/10.1111/gcb.13365

DeAngelis, K. M., Pold, G., Topçuoğlu, B. D., van Diepen, L. T. A., Varney, R. M., Blanchard, J. L., Melillo, J., & Frey, S. D. (2015). Long-term forest soil warming alters microbial communities in temperate forest soils. *Frontiers in Microbiology*, *6*(104), 104. https://doi.org/10.3389/fmicb.2015.00104

Del Campo, J., Sieracki, M. E., Molestina, R., Keeling, P., Massana, R., & Ruiz-Trillo, I. (2014). The others: Our biased perspective of eukaryotic genomes. *Trends in Ecology and Evolution*, *29*(5), 252–259. https://doi.org/10.1016/j.tree.2014.03.006

Delafont, V., Samba-Louaka, A., Bouchon, D., Moulin, L., & Héchard, Y. (2015). Shedding light on microbial dark matter: A TM6 bacterium as natural endosymbiont of a free-living amoeba. *Environmental Microbiology Reports*, *7*(6), 970–978. https://doi.org/10.1111/1758-2229.12343

Donhauser, J., & Frey, B. (2018). Alpine soil microbial ecology in a changing world. *FEMS Microbiology Ecology*, *94*(9), fiy099. https://doi.org/10.1093/femsec/fiy099

Donhauser, J., Niklaus, P. A., Rousk, J., Larose, C., & Frey, B. (2020). Temperatures beyond the community optimum promote the dominance of heat-adapted, fast growing and stress resistant bacteria in alpine soils. *Soil Biology and Biochemistry*, 107873. https://doi.org/https://doi.org/10.1016/j.soilbio.2020.107873

Dudek, N. K., Sun, C. L., Burstein, D., Kantor, R. S., Aliaga Goltsman, D. S., Bik, E. M., Thomas, B. C., Banfield, J. F., & Relman, D. A. (2017). Novel Microbial Diversity and Functional Potential in the Marine Mammal Oral Microbiome. *Current Biology*, *27*(24), 3752-3762.e6. https://doi.org/10.1016/j.cub.2017.10.040

Edgar, R. C. (2013). UPARSE: highly accurate OTU sequences from microbial amplicon reads. *Nature Methods*, *10*(10), 996–998. https://doi.org/10.1038/nmeth.2604

Eloe-Fadrosh, E. A., Ivanova, N. N., Woyke, T., & Kyrpides, N. C. (2016). Metagenomics uncovers gaps in amplicon-based detection of microbial diversity. *Nature Microbiology*, *1*(February), 15032. https://doi.org/10.1038/nmicrobiol.2015.32

Ferenci, T. (2016). Trade-off Mechanisms Shaping the Diversity of Bacteria. *Trends in Microbiology*, *24*(3), 209–223. https://doi.org/10.1016/j.tim.2015.11.009

Fierer, N., Bradford, M. A., & Jackson, R. B. (2007). TOWARD AN ECOLOGICAL CLASSIFICATION OF SOIL BACTERIA. *Ecology*, *88*(6), 1354–1364. https://doi.org/doi:10.1890/05-1839

Frey, B., Rime, T., Phillips, M., Stierli, B., Hajdas, I., Widmer, F., & Hartmann, M. (2016). Microbial diversity in European alpine permafrost and active layers. *FEMS Microbiology Ecology*, *92*(3),

fiw018. https://doi.org/10.1093/femsec/fiw018

Galperin, M. Y., Makarova, K. S., Wolf, Y. I., & Koonin, E. V. (2015). Expanded Microbial genome coverage and improved protein family annotation in the COG database. *Nucleic Acids Research*, *43*(D1), D261–D269. https://doi.org/10.1093/nar/gku1223

Gobiet, A., Kotlarski, S., Beniston, M., Heinrich, G., Rajczak, J., & Stoffel, M. (2014). 21st century climate change in the European Alps—A review. *Science of the Total Environment*, *493*, 1138–1151. https://doi.org/http://dx.doi.org/10.1016/j.scitotenv.2013.07.050

Gudelj, I., Weitz, J. S., Ferenci, T., Claire Horner-Devine, M., Marx, C. J., Meyer, J. R., & Forde, S. E. (2010). An integrative approach to understanding microbial diversity: From intracellular mechanisms to community structure. *Ecology Letters*, *13*(9), 1073–1084. https://doi.org/10.1111/j.1461-0248.2010.01507.x

Guenet, B., Juarez, S., Bardoux, G., Pouteau, V., Cheviron, N., Marrauld, C., Abbadie, L., & Chenu, C. (2011). Metabolic capacities of microorganisms from a long-term bare fallow. *Applied Soil Ecology*, *51*(1), 87–93. https://doi.org/10.1016/j.apsoil.2011.07.006

Guo, G., Kong, W., Liu, J., Zhao, J., Du, H., Zhang, X., & Xia, P. (2015). Diversity and distribution of autotrophic microbial community along environmental gradients in grassland soils on the Tibetan Plateau. *Applied Microbiology and Biotechnology*, *99*(20), 8765–8776. https://doi.org/10.1007/s00253-015-6723-x

Hagedorn, F., Gavazov, K., & Alexander, J. M. (2019). Above- and belowground linkages shape responses of mountain vegetation to climate change. *Science*, *365*(6458), 1119–1123. https://doi.org/10.1126/science.aax4737

Hagedorn, F., Martin, M., Rixen, C., Rusch, S., Bebi, P., Zürcher, A., Siegwolf, R. T. W., Wipf, S., Escape, C., Roy, J., & Hättenschwiler, S. (2010). Short-term responses of ecosystem carbon fluxes to experimental soil warming at the Swiss alpine treeline. *Biogeochemistry*, *97*(1), 7–19. https://doi.org/10.1007/s10533-009-9297-9

Hartman, D. J., Surin, B. P., Dixon, N. E., Hoogenraad, N. J., & Høj, P. B. (1993). Substoichiometric amounts of the molecular chaperones GroEL and GroES prevent thermal denaturation and aggregation of mammalian mitochondrial malate dehydrogenase in vitro. *Proceedings of the National Academy of Sciences of the United States of America*, *90*(6), 2276–2280. https://doi.org/10.1073/pnas.90.6.2276

Hatzenpichler, R. (2012). Diversity, physiology, and niche differentiation of ammonia-oxidizing archaea. *Applied and Environmental Microbiology*, *78*(21), 7501–7510. https://doi.org/10.1128/AEM.01960-12

He, J., Hu, H., & Zhang, L. (2012). Soil Biology & Biochemistry Current insights into the autotrophic thaumarchaeal ammonia oxidation in acidic soils. *Soil Biology and Biochemistry*, *55*, 146–154.

https://doi.org/10.1016/j.soilbio.2012.06.006

Horcajo, P., De Pedro, M. A., & Cava, F. (2012). Peptidoglycan plasticity in bacteria: Stress-induced peptidoglycan editing by noncanonical D-amino acids. *Microbial Drug Resistance*, *18*(3), 306–313. https://doi.org/10.1089/mdr.2012.0009

Hu, Y., Zheng, Q., & Wanek, W. (2017). Flux Analysis of Free Amino Sugars and Amino Acids in Soils by Isotope Tracing with a Novel Liquid Chromatography/High Resolution Mass Spectrometry Platform. *Analytical Chemistry*, *89*(17), 9192–9200. https://doi.org/10.1021/acs.analchem.7b01938

Huang, Y., Guenet, B., Ciais, P., Janssens, I. A., Soong, J. L., Wang, Y., Goll, D., Blagodatskaya, E., & Huang, Y. (2018). ORCHIMIC (v1.0), a microbe-mediated model for soil organic matter decomposition. *Geoscientific Model Development*, *11*(6), 2111–2138. https://doi.org/10.5194/gmd-11-2111-2018

Huerta-Cepas, J., Szklarczyk, D., Forslund, K., Cook, H., Heller, D., Walter, M. C., Rattei, T., Mende, D. R., Sunagawa, S., Kuhn, M., Jensen, L. J., Von Mering, C., & Bork, P. (2016). EGGNOG 4.5: A hierarchical orthology framework with improved functional annotations for eukaryotic, prokaryotic and viral sequences. *Nucleic Acids Research*, *44*(D1), D286–D293. https://doi.org/10.1093/nar/gkv1248

Jacquiod, S., Stenbæk, J., Santos, S. S., Winding, A., Sørensen, S. J., & Priemé, A. (2016). Metagenomes provide valuable comparative information on soil microeukaryotes. *Research in Microbiology*, *167*(5), 436–450. https://doi.org/10.1016/j.resmic.2016.03.003

Jurburg, S. D., Nunes, I., Brejnrod, A., Jacquiod, S., Priemé, A., Sørensen, S. J., Van Elsas, J. D., & Salles, J. F. (2017). Legacy effects on the recovery of soil bacterial communities from extreme temperature perturbation. *Frontiers in Microbiology*, *8*(SEP), 1832. https://doi.org/10.3389/fmicb.2017.01832

Jurburg, S. D., Nunes, I., Stegen, J. C., Le Roux, X., Priemé, A., Sørensen, S. J., & Salles, J. F. (2017). Autogenic succession and deterministic recovery following disturbance in soil bacterial communities. *Scientific Reports*, *7*, 45691. https://doi.org/10.1038/srep45691

Kaiser, C., Franklin, O., Dieckmann, U., & Richter, A. (2014). Microbial community dynamics alleviate stoichiometric constraints during litter decay. *Ecology Letters*, *17*(6), 680–690. https://doi.org/10.1111/ele.12269

Kerfahi, D., Tripathi, B. M., Dong, K., Kim, M., Kim, H., Ferry Slik, J. W., Go, R., & Adams, J. M. (2019). From the High Arctic to the Equator: Do Soil Metagenomes Differ According to Our Expectations? *Microbial Ecology*, *77*(1), 168–185. https://doi.org/10.1007/s00248-018-1215-z

Kerfahi, D., Tripathi, B. M., Porazinska, D. L., Park, J., Go, R., & Adams, J. M. (2016). Do tropical rain forest soils have greater nematode diversity than High Arctic tundra? A metagenetic comparison of Malaysia and Svalbard. *Global Ecology and Biogeography*, *25*(6), 716–728. https://doi.org/10.1111/geb.12448

Kindler, R., Miltner, A., Richnow, H. H., & Kästner, M. (2006). Fate of gram-negative bacterial biomass in soil - Mineralization and contribution to SOM. *Soil Biology and Biochemistry*, *38*(9), 2860–2870. https://doi.org/10.1016/j.soilbio.2006.04.047

Klindworth, A., Pruesse, E., Schweer, T., Peplies, J., Quast, C., Horn, M., & Glöckner, F. O. (2013). Evaluation of general 16S ribosomal RNA gene PCR primers for classical and next-generation sequencing-based diversity studies. *Nucleic Acids Research*, *41*(1), 1–11. https://doi.org/10.1093/nar/gks808

Koonin, E. V., & Aravind, L. (1998). Genomics: Re-evaluation of translation machinery evolution. *Current Biology*, *8*(8), 266–269. https://doi.org/10.1016/s0960-9822(98)70169-1

Kuzyakov, Y., & Mason-Jones, K. (2018). Viruses in soil: Nano-scale undead drivers of microbial life, biogeochemical turnover and ecosystem functions. *Soil Biology and Biochemistry*, *127*(March), 305–317. https://doi.org/10.1016/j.soilbio.2018.09.032

Lauro, F. M., McDougald, D., Thomas, T., Williams, T. J., Egan, S., Rice, S., DeMaere, M. Z., Ting, L., Ertan, H., Johnson, J., Ferriera, S., Lapidus, A., Anderson, I., Kyrpides, N., Munk, A. C., Detter, C., Han, C. S., Brown, M. V, Robb, F. T., … Cavicchioli, R. (2009). The genomic basis of trophic strategy in marine bacteria. *Proceedings of the National Academy of Sciences*, *106*(37), 15527–15533. https://doi.org/10.1073/pnas.0903507106

Le, P. T., Makhalanyane, T. P., Guerrero, L. D., Vikram, S., De Peer, Y. Van, & Cowan, D. A. (2016). Comparative metagenomic analysis reveals mechanisms for stress response in hypoliths from extreme hyperarid deserts. *Genome Biology and Evolution*, *8*(9), 2737–2747. https://doi.org/10.1093/gbe/evw189

Lehmann, J., & Kleber, M. (2015). The contentious nature of soil organic matter. *Nature*, *528*(7580), 60–68. https://doi.org/10.1038/nature16069

Li, D., Liu, C. M., Luo, R., Sadakane, K., & Lam, T. W. (2015). MEGAHIT: An ultra-fast single-node solution for large and complex metagenomics assembly via succinct de Bruijn graph. *Bioinformatics*, *31*(10), 1674–1676. https://doi.org/10.1093/bioinformatics/btv033

Li, H. (2013). *Aligning sequence reads, clone sequences and assembly contigs with BWA-MEM*. *00*(00), 1–3. http://arxiv.org/abs/1303.3997

Li, Y., Lin, Q., Wang, S., Li, X., Liu, W., Luo, C., Zhang, Z., Zhu, X., Jiang, L., & Li, X. (2016). Soil bacterial community responses to warming and grazing in a Tibetan alpine meadow. *FEMS Microbiology Ecology*, *92*(1). https://doi.org/10.1093/femsec/fiv152

Liao, Y., Smyth, G. K., & Shi, W. (2014). FeatureCounts: An efficient general purpose program for assigning sequence reads to genomic features. *Bioinformatics*, *30*(7), 923–930. https://doi.org/10.1093/bioinformatics/btt656

Love, M. I., Huber, W., & Anders, S. (2014). Moderated estimation of fold change and dispersion for

RNA-seq data with DESeq2. *Genome Biology*, *15*(12), 550. https://doi.org/10.1186/s13059-014-0550-8

Lulakova, P., Perez-Mon, C., Santruckova, H., Ruethi, J., & Frey, B. (2019). High-Alpine Permafrost and Active-Layer Soil Microbiomes Differ in Their Response to Elevated Temperatures. *Frontiers in Microbiology*, *10*, 668. https://doi.org/10.3389/fmicb.2019.00668

Luo, C., Rodriguez-R, L. M., Johnston, E. R., Wu, L., Cheng, L., Xue, K., Tu, Q., Deng, Y., He, Z., Shi, J. Z., Yuan, M. M., Sherry, R. A., Li, D., Luo, Y., Schuur, E. A. G., Chain, P., Tiedje, J. M., Zhou, J., & Konstantinidis, K. T. (2014). Soil microbial community responses to a decade of warming as revealed by comparative metagenomics. *Applied and Environmental Microbiology*, *80*(5), 1777–1786. https://doi.org/10.1128/AEM.03712-13

Maharjan, R., Nilsson, S., Sung, J., Haynes, K., Beardmore, R. E., Hurst, L. D., Ferenci, T., & Gudelj, I. (2013). The form of a trade-off determines the response to competition. *Ecology Letters*, *16*(10), 1267–1276. https://doi.org/10.1111/ele.12159

Mathé, C., Sagot, M. F., Schiex, T., & Rouzé, P. (2002). Current methods of gene prediction, their strengths and weaknesses. *Nucleic Acids Research*, *30*(19), 4103–4117. https://doi.org/10.1093/nar/gkf543

McLean, J. S., Lombardo, M. J., Badger, J. H., Edlund, A., Novotny, M., Yee-Greenbaum, J., Vyahhi, N., Hall, A. P., Yang, Y., Dupont, C. L., Ziegler, M. G., Chitsaz, H., Allen, A. E., Yooseph, S., Tesler, G., Pevzner, P. A., Friedman, R. M., Nealson, K. H., Venter, J. C., & Lasken, R. S. (2013). Candidate phylum TM6 genome recovered from a hospital sink biofilm provides genomic insights into this uncultivated phylum. *Proceedings of the National Academy of Sciences of the United States of America*, *110*(26). https://doi.org/10.1073/pnas.1219809110

McMurdie, P. J., & Holmes, S. (2013). phyloseq: An R Package for Reproducible Interactive Analysis and Graphics of Microbiome Census Data. *PLOS ONE*, *8*(4), e61217. https://doi.org/10.1371/journal.pone.0061217

Melillo, J. M., Frey, S. D., DeAngelis, K. M., Werner, W. J., Bernard, M. J., Bowles, F. P., Pold, G., Knorr, M. A., & Grandy, A. S. (2017). Long-term pattern and magnitude of soil carbon feedback to the climate system in a warming world. *Science*, *358*(6359), 101–105. https://doi.org/10.1126/science.aan2874

Melillo, J. M., Steudler, P. A., Aber, J. D., Newkirk, K., Lux, H., Bowles, F. P., Catricala, C., Magill, A., Ahrens, T., & Morrisseau, S. (2002). Soil Warming and Carbon-Cycle Feedbacks to the Climate System. *Science*, *298*(5601), 2173–2176. https://doi.org/10.1126/science.1074153

Mendoza, J. A., Warren, T., & Dulin, P. (1996). The ATPase activity of chaperonin GroEL is highly stimulated at elevated temperatures. *Biochemical and Biophysical Research Communications*, *229*(1), 271–274. https://doi.org/10.1006/bbrc.1996.1791

Mooshammer, M., Hofhansl, F., Frank, A. H., Wanek, W., Hämmerle, I., Leitner, S., Schnecker, J., Wild, B., Watzka, M., Keiblinger, K. M., Zechmeister-Boltenstern, S., & Richter, A. (2017). Decoupling of microbial carbon, nitrogen, and phosphorus cycling in response to extreme temperature events. *Science Advances*, *3*(5), e1602781. https://doi.org/10.1126/sciadv.1602781

Mooshammer, M., Wanek, W., Hämmerle, I., Fuchslueger, L., Hofhansl, F., Knoltsch, A., Schnecker, J., Takriti, M., Watzka, M., Wild, B., Keiblinger, K. M., Zechmeister-Boltenstern, S., & Richter, A. (2014b). Adjustment of microbial nitrogen use efficiency to carbon:Nitrogen imbalances regulates soil nitrogen cycling. *Nature Communications*, *5*, 1–7. https://doi.org/10.1038/ncomms4694

Mooshammer, M., Wanek, W., Zechmeister-Boltenstern, S., & Richter, A. (2014a). Stoichiometric imbalances between terrestrial decomposer communities and their resources: Mechanisms and implications of microbial adaptations to their resources. *Frontiers in Microbiology*, *5*(FEB), 1–10. https://doi.org/10.3389/fmicb.2014.00022

Nielsen, U. N., Ayres, E., Wall, D. H., Li, G., Bardgett, R. D., Wu, T., & Garey, J. R. (2014). Global-scale patterns of assemblage structure of soil nematodes in relation to climate and ecosystem properties. *Global Ecology and Biogeography*, *23*(9), 968–978. https://doi.org/10.1111/geb.12177

Norman, R. J., & Stucki, J. W. (1981). The Determination of Nitrate and Nitrite in Soil Extracts by Ultraviolet Spectrophotometry. *Soil Science Society of America Journal*, *45*(2), 347–353. https://doi.org/10.2136/sssaj1981.03615995004500020024x

Noronha, M. F., Lacerda Júnior, G. V., Gilbert, J. A., & de Oliveira, V. M. (2017). Taxonomic and functional patterns across soil microbial communities of global biomes. *Science of the Total Environment*, *609*, 1064–1074. https://doi.org/10.1016/j.scitotenv.2017.07.159

Nunes, I., Jurburg, S., Jacquiod, S., Brejnrod, A., Falcão Salles, J., Priemé, A., & Sørensen, S. J. (2018). Soil bacteria show different tolerance ranges to an unprecedented disturbance. *Biology and Fertility of Soils*, *54*(2), 189–202. https://doi.org/10.1007/s00374-017-1255-4

Ogwu, M. C., Kerfahi, D., Song, H. K., Dong, K., Seo, H., Lim, S., Srinivasan, S., Kim, M. K., Waldman, B., & Adams, J. M. (2019). Changes in soil taxonomic and functional diversity resulting from gamma irradiation. *Scientific Reports*, *9*(1), 1–13. https://doi.org/10.1038/s41598-019-44441-7

Oksanen, J., Kindt, R., & Legendre, P. (2013). *The Vegan Package: Community Ecology Package 2007*.

Parks, D. H., Imelfort, M., Skennerton, C. T., Hugenholtz, P., & Tyson, G. W. (2015). CheckM: Assessing the quality of microbial genomes recovered from isolates, single cells, and metagenomes. *Genome Research*, *25*(7), 1043–1055. https://doi.org/10.1101/gr.186072.114

Perez-Mon, C., Frey, B., & Frossard, A. (2020). *Functional and Structural Responses of Arctic and Alpine Soil Prokaryotic and Fungal Communities Under Freeze-Thaw Cycles of Different Frequencies*. *11*(May), 1–14. https://doi.org/10.3389/fmicb.2020.00982

Pignatelli, M., Aparicio, G., Blanquer, I., Hernández, V., Moya, A., & Tamames, J. (2008). Metagenomics

reveals our incomplete knowledge of global diversity. *Bioinformatics*, *24*(18), 2124–2125. https://doi.org/10.1093/bioinformatics/btn355

Pruesse, E., Peplies, J., & Glöckner, F. O. (2012). SINA: Accurate high-throughput multiple sequence alignment of ribosomal RNA genes. *Bioinformatics*, *28*(14), 1823–1829. https://doi.org/10.1093/bioinformatics/bts252

Quast, C., Pruesse, E., Yilmaz, P., Gerken, J., Schweer, T., Yarza, P., Peplies, J., & Glöckner, F. O. (2013). The SILVA ribosomal RNA gene database project: improved data processing and web-based tools. *Nucleic Acids Research*, *41*(Database issue), D590–D596. https://doi.org/10.1093/nar/gks1219

R Core Team. (2018). *A Language and Environment for Statistical Computing*. R Foundation for Statistical Computing.

Ratkowsky, D. A., Lowry, R. K., McMeekin, T. A., Stokes, A. N., & Chandler, R. E. (1983). Model for bacterial culture growth rate throughout the entire biokinetic temperature range. *Journal of Bacteriology*, *154*(3), 1222–1226. https://www.ncbi.nlm.nih.gov/pubmed/6853443

Rime, T., Hartmann, M., & Frey, B. (2016) Potential sources of microbial colonizers in inital soil ecosystem after retreat of an Alpine glacier. *ISME Journal*, *10*(7), 1625–1641. https://doi.org/10.1038/ismej.2015.238

Rinke, C., Schwientek, P., Sczyrba, A., Ivanova, N. N., Anderson, I. J., Cheng, J.-F., Darling, A., Malfatti, S., Swan, B. K., Gies, E. A., Dodsworth, J. A., Hedlund, B. P., Tsiamis, G., Sievert, S. M., Liu, W.-T., Eisen, J. A., Hallam, S. J., Kyrpides, N. C., Stepanauskas, R., … Woyke, T. (2013). Insights into the phylogeny and coding potential of microbial dark matter. *Nature*, *499*(7459), 431–437. https://doi.org/10.1038/nature12352

Rinnan, R., Michelsen, A., Baath, E., & Jonasson, S. (2007). Fifteen years of climate change manipulations alter soil microbial communities in a subarctic heath ecosystem. *Global Change Biology*, *13*(1), 28–39. https://doi.org/10.1111/j.1365-2486.2006.01263.x

Rinnan, R., Rousk, J., Yergeau, E., Kowalchuk, G. A., & Bååth, E. (2009). Temperature adaptation of soil bacterial communities along an Antarctic climate gradient: Predicting responses to climate warming. *Global Change Biology*, *15*(11), 2615–2625. https://doi.org/10.1111/j.1365-2486.2009.01959.x

Romero-Olivares, A. L., Allison, S. D., & Treseder, K. K. (2017). Soil microbes and their response to experimental warming over time: A meta-analysis of field studies. *Soil Biology and Biochemistry*, *107*, 32–40. https://doi.org/10.1016/j.soilbio.2016.12.026

Ron, E. Z. (2013). Bacterial Stress Response. In E. Rosenberg, E. F. DeLong, S. Lory, E. Stackebrandt, & F. Thompson (Eds.), *The Prokaryotes: Prokaryotic Physiology and Biochemistry* (pp. 589–603). Springer Berlin Heidelberg. https://doi.org/10.1007/978-3-642-30141-4_79

Rousk, J., Frey, S. D., & Bååth, E. (2012). Temperature adaptation of bacterial communities in experimentally warmed forest soils. *Global Change Biology*, *18*(10), 3252–3258.

https://doi.org/10.1111/j.1365-2486.2012.02764.x

Rousk, K., Michelsen, A., & Rousk, J. (2016). Microbial control of soil organic matter mineralization responses to labile carbon in subarctic climate change treatments. *Global Change Biology*, *22*(12), 4150–4161. https://doi.org/10.1111/gcb.13296

Rui, J., Li, J., Wang, S., An, J., Liu, W. tso, Lin, Q., Yang, Y., He, Z., & Li, X. (2015). Responses of bacterial communities to simulated climate changes in alpine meadow soil of the Qinghai-Tibet plateau. *Applied and Environmental Microbiology*, *81*(17), 6070–6077. https://doi.org/10.1128/AEM.00557-15

Santillan, E., Seshan, H., Constancias, F., & Wuertz, S. (2019). Trait-based life-history strategies explain succession scenario for complex bacterial communities under varying disturbance. *Environmental Microbiology*, *21*(10), 3751–3764. https://doi.org/10.1111/1462-2920.14725

Schleppi, P., Bucher-Wallin, I., Hagedorn, F., & Körner, C. (2012). Increased nitrate availability in the soil of a mixed mature temperate forest subjected to elevated CO 2 concentration (canopy FACE). *Global Change Biology*, *18*(2), 757–768. https://doi.org/10.1111/j.1365-2486.2011.02559.x

Schostag, M. D., Anwar, M. Z., Jacobsen, C. S., Larose, C., Vogel, T. M., Maccario, L., Jacquiod, S., Faucherre, S., & Priemé, A. (2019). Transcriptomic responses to warming and cooling of an Arctic tundra soil microbiome. *BioRxiv*, 599233. https://doi.org/10.1101/599233

Schostag, M. D., Priemé, A., Jacquiod, S., Russel, J., Ekelund, F., & Jacobsen, C. S. (2019). Bacterial and protozoan dynamics upon thawing and freezing of an active layer permafrost soil. *The ISME Journal*, *13*(5), 1345–1359. https://doi.org/10.1038/s41396-019-0351-x

Sherrill-Mix, S. (2019). *taxonomizr: Functions to Work with NCBI Accessions and Taxonomy*. https://cran.r-project.org/package=taxonomizr

Song, H. K., Shi, Y., Yang, T., Chu, H., He, J. S., Kim, H., Jablonski, P., & Adams, J. M. (2019). Environmental filtering of bacterial functional diversity along an aridity gradient. *Scientific Reports*, *9*(1), 1–10. https://doi.org/10.1038/s41598-018-37565-9

Soong, J. L., Fuchslueger, L., Marañon-Jimenez, S., Torn, M. S., Janssens, I. A., Penuelas, J., & Richter, A. (2020). Microbial carbon limitation: The need for integrating microorganisms into our understanding of ecosystem carbon cycling. *Global Change Biology*, *26*(4), 1953–1961. https://doi.org/10.1111/gcb.14962

Steinbauer, M. J., Grytnes, J.-A., Jurasinski, G., Kulonen, A., Lenoir, J., Pauli, H., Rixen, C., Winkler, M., Bardy-Durchhalter, M., Barni, E., Bjorkman, A. D., Breiner, F. T., Burg, S., Czortek, P., Dawes, M. A., Delimat, A., Dullinger, S., Erschbamer, B., Felde, V. A., … Wipf, S. (2018). Accelerated increase in plant species richness on mountain summits is linked to warming. *Nature*, *556*(7700), 231–234. https://doi.org/10.1038/s41586-018-0005-6

Štursová, M., Žifčáková, L., Leigh, M. B., Burgess, R., & Baldrian, P. (2012). Cellulose utilization in forest

litter and soil: identification of bacterial and fungal decomposers. *FEMS Microbiology Ecology*, *80*(3), 735–746. https://doi.org/10.1111/j.1574-6941.2012.01343.x

Tao, X., Feng, J., Yang, Y., Wang, G., Tian, R., Fan, F., Ning, D., Bates, C. T., Hale, L., Yuan, M. M., Wu, L., Gao, Q., Lei, J., Schuur, E. A. G., Yu, J., Bracho, R., Luo, Y., Konstantinidis, K. T., Johnston, E. R., … Zhou, J. (2020). Winter warming in Alaska accelerates lignin decomposition contributed by Proteobacteria. *Microbiome*, *8*(1), 1–12. https://doi.org/10.1186/s40168-020-00838-5

Tu, Q., Lin, L., Cheng, L., Deng, Y., & He, Z. (2018). NCycDB: a curated integrative database for fast and accurate metagenomic profiling of nitrogen cycling genes. *Bioinformatics*, *35*(6), 1040–1048. https://doi.org/10.1093/bioinformatics/bty741

van Gestel, N. C., Reischke, S., & Bååth, E. (2013). Temperature sensitivity of bacterial growth in a hot desert soil with large temperature fluctuations. *Soil Biology & Biochemistry*, *65*, 180–185. https://doi.org/https://doi.org/10.1016/j.soilbio.2013.05.016

Vaser, R., Pavlović, D., & Šikić, M. (2016). SWORD - A highly efficient protein database search. *Bioinformatics*, *32*(17), i680–i684. https://doi.org/10.1093/bioinformatics/btw445

Wang, Q., Garrity, G. M., Tiedje, J. M., & Cole, J. R. (2007). Naïve Bayesian Classifier for Rapid Assignment of rRNA Sequences into the New Bacterial Taxonomy. *Applied and Environmental Microbiology*, *73*(16), 5261–5267. https://doi.org/10.1128/aem.00062-07

Wang, X., Wang, C., Cotrufo, M. F., Sun, L., Jiang, P., Liu, Z., & Bai, E. (2020). Elevated temperature increases the accumulation of microbial necromass nitrogen in soil via increasing microbial turnover. *Global Change Biology*, *May*, 1–13. https://doi.org/10.1111/gcb.15206

Wickham, H. (2009). *ggplot2: Elegant Graphics for Data Analysis*. Springer Publishing Company, Incorporated.

Wilke, A., Harrison, T., Wilkening, J., Field, D., Glass, E. M., Kyrpides, N., Mavrommatis, K., & Meyer, F. (2012). The M5nr: a novel non-redundant database containing protein sequences and annotations from multiple sources and associated tools. *BMC Bioinformatics*, *13*(1), 141. https://doi.org/10.1186/1471-2105-13-141

Wu, J., Xiong, J., Hu, C., Shi, Y., Wang, K., & Zhang, D. (2015). Temperature sensitivity of soil bacterial community along contrasting warming gradient. *Applied Soil Ecology*, *94*, 40–48. https://doi.org/10.1016/j.apsoil.2015.04.018

Xu, X., Thornton, P. E., & Post, W. M. (2013). A global analysis of soil microbial biomass carbon, nitrogen and phosphorus in terrestrial ecosystems. *Global Ecology and Biogeography*, *22*(6), 737–749. https://doi.org/10.1111/geb.12029

Yang, Y., Gao, Y., Wang, S., Xu, D., Yu, H., Wu, L., Lin, Q., Hu, Y., Li, X., He, Z., Deng, Y., & Zhou, J. (2014). The microbial gene diversity along an elevation gradient of the Tibetan grassland. *Isme Journal*, *8*(2), 430–440. https://doi.org/10.1038/ismej.2013.146

Yeoh, Y. K., Sekiguchi, Y., Parks, D. H., & Hugenholtz, P. (2015). Comparative Genomics of Candidate Phylum TM6 Suggests That Parasitism Is Widespread and Ancestral in This Lineage. *Molecular Biology and Evolution*, *33*(4), 915–927. https://doi.org/10.1093/molbev/msv281

Yu, C., Han, F., & Fu, G. (2019). Effects of 7 years experimental warming on soil bacterial and fungal community structure in the Northern Tibet alpine meadow at three elevations. *Science of the Total Environment*, *655*, 814–822. https://doi.org/10.1016/j.scitotenv.2018.11.309

Yuan, Y., Si, G., Li, W., & Zhang, G. (2015). Altitudinal Distribution of Ammonia-Oxidizing Archaea and Bacteria in Alpine Grassland Soils Along the South-Facing Slope of Nyqentangula Mountains, Central Tibetan Plateau. *Geomicrobiology Journal*, *32*(1), 77–88. https://doi.org/10.1080/01490451.2014.925013

Yue, H., Wang, M., Wang, S., Gilbert, J. A., Sun, X., Wu, L., Lin, Q., Hu, Y., Li, X., He, Z., Zhou, J., & Yang, Y. (2015). The microbe-mediated mechanisms affecting topsoil carbon stock in Tibetan grasslands. *ISME Journal*, *9*(9), 2012–2020. https://doi.org/10.1038/ismej.2015.19

Zhang, B., Chen, S. Y., Zhang, J. F., He, X. Y., Liu, W. J., Zhao, Q., Zhao, L., & Tian, C. J. (2015). Depth-related responses of soil microbial communities toexperimental warming in an alpine meadow on the Qinghai-Tibet Plateau. *European Journal of Soil Science*, *66*(3), 496–504. https://doi.org/10.1111/ejss.12240

Zhang, X., Johnston, E. R., Li, L., Konstantinidis, K. T., & Han, X. (2017). Experimental warming reveals positive feedbacks to climate change in the Eurasian Steppe. *The ISME Journal*, *11*(4), 885–895. https://doi.org/10.1038/ismej.2016.180

Zhang, Y., Lu, Z., Liu, S., Yang, Y., He, Z., Ren, Z., Zhou, J., & Li, D. (2013). Geochip-based analysis of microbial communities in alpine meadow soils in the Qinghai-Tibetan plateau. *BMC Microbiology*, *13*(1). https://doi.org/10.1186/1471-2180-13-72

Zhou, J., Xue, K., Xie, J., Deng, Y., Wu, L., Cheng, X., Fei, S., Deng, S., He, Z., Van Nostrand, J. D., & Luo, Y. (2012). Microbial mediation of carbon-cycle feedbacks to climate warming. *Nature Climate Change*, *2*(2), 106–110. https://doi.org/10.1038/nclimate1331

Zhu, A., Ibrahim, J. G., & Love, M. I. (2019). Heavy-Tailed prior distributions for sequence count data: Removing the noise and preserving large differences. *Bioinformatics*, *35*(12), 2084–2092. https://doi.org/10.1093/bioinformatics/bty895

Zumsteg, A., Baath, E., Stierli, B., Zeyer, J., & Frey, B. (2013). Bacterial and fungal community responses to reciprocal soil transfer along a temperature and soil moisture gradient in a glacier forefield. *Soil Biology & Biochemistry*, *61*, 121–132. https://doi.org/10.1016/j.soilbio.2013.02.017

Figure captions

Figure 1: Temperature effects on functional and structural diversity. Observed richness of functional genes identified with eggNOG, CAZy and NCycDB and of ribosomal RNA genes (mean ± SD, n = 3). Different letters indicate a significant ($P < 0.05$) difference between temperatures as assessed by one-way analysis of variance (ANOVA) followed by a Tukey HSD post-hoc test. T0 = time 0 (pre-experiment control).

Figure 2: Temperature effects on functional gene structures and microbial community structures. Principal coordinate analysis (PCoA) of functional gene structures of genes annotated with the eggNOG (a), CAZy (a), NcycDB (c), and microbial community structures based on 16S and 18S rRNA genes (d). Ordinations were based on Bray–Curtis dissimilarities of relative abundances. The variation explained by each PCoA axis is given in brackets. Vectors represent regression of soil chemical and bacterial growth parameters against the PCoA ordination scores. Solid vectors with bold labels represent significant correlations ($P < 0.05$). TC = total carbon, TN = total nitrogen, DOC = dissolved organic carbon, DON = dissolved organic nitrogen, T_{opt}= optimum temperature for bacterial growth, T_{min}= minimum temperature for bacterial growth, growth 4 = bacterial growth rates at 4 °C, growth 35 = bacterial growth rates at 35 °C, T0 = time 0 (pre-experiment control).

Figure 3: Changes in taxonomic composition with temperature based on functional and ribosomal genes. Relative abundance at the phylum level based on functional genes identified with the md5nr/eggNOG and CAZy, as well as based on ribosomal genes (16S and 18S rRNA genes extracted from metagenomes and

16S rRNA amplicon sequencing). Phylum names are given according to both the SILVA taxonomy (used for taxonomic classification of ribosomal genes) and according to the NCBI taxonomy (used for taxonomic classification of functional genes annotated with CAZy and md5nr/eggNOG. Bars represent the mean of three replicates. Groups with abundance < 0.01 are summed as Others. T0 = time 0 (pre-experiment control).

Figure 4: General impact of temperature on microbial functions. Log_2-fold changes (LFC) in functional genes annotated with eggNOG aggregated over functional categories at 35 °C relative to 4 °C (mean ± SD, n = 3). Significant LFCs with $p_{adj.} < 0.01$ are shown. At 15 and 25 °C none of the categories were significant.

Figure 5: General impact of temperature on microbial functions at the function level. Bars represent log_2-fold changes (LFC) in functional genes annotated with eggNOG at 15 °C (top right), at 25 °C (bottom left) and at 35 °C (bottom right) relative to 4 °C (mean ± SD, n = 3). Functions with a significant LFC with $p_{adj.} < 0.01$ are shown. At 25 and at 35 °C, the 75 most abundant functions are shown. Points depict LFCs for different genes in the metagenomes annotated with the same function. The size of the points indicates the average abundance of the genes across the whole dataset (raw count data normalized by the size factor derived from the DESeq2 analysis).

Figure 6. Impact of temperature on C-cycling genes. Bars represent log_2-fold changes (LFC) in C-cycling genes annotated with CAZy aggregated over CAZy families at 15 °C (top left), at 25 °C (bottom left) and at 35 °C (right) relative to 4 °C (mean ± SD, n = 3). Functions with a significant LFC with $p_{adj.} < 0.01$ are shown. At 35 °C the 75 most abundant functions are shown. Points depict LFCs individually for different genes in the metagenomes annotated with the same CAZy family. The size of the points indicates the average abundance of the genes across the whole dataset (raw count data normalized by the size factor derived from the DESeq2 analysis). Colors indicate the substrate category that enzymes from the respective CAZy family degrade, according to recalcitrance or association of a CAZy family with murein degradation and modification of membranes and cell walls. Grey bars represent genes that could not be assigned to these categories. Arrows additionally highlight CAZy families associated with murein degradation and modification of membranes and cell walls at 35 °C.

Figure 7: Impact of temperature on N-cycling genes. Bars represent log_2-fold changes (LFC) in N-cycling genes annotated with NCycDB, aggregated over N-cycling genes at 25 °C (top) and at 35 °C (bottom) relative to 4 °C (mean ± SD, n = 3). Functions with a significant LFC with $p_{adj.} < 0.05$ are shown. At 15 °C no significant LFCs were detected. Points depict LFCs individually for different genes in the metagenomes

annotated with the same N-cycling gene. The size of the points indicates the average abundance of the genes across the whole dataset (raw count data normalized by the size factor derived from the DESeq2 analysis).

Chemical variables									Bacterial growth parameters			
	TC [%]	TN [%]	C:N	DOC [mg/g]	DON [mg/g]	DOC:DON	NH_4^+ [ug/g]	NO_3^- [ug/g]	4 °C	35°C	T_{min}	T_{opt}
T0	0.47 ± 0.02	0.05 ± 0.00	10.3 ± 0.1^{AB}	0.13 ± 0.02	0.02 ± 0.00^{A}	5.9 ± 0.5^{A}	1.55 ± 0.15^{A}	62.70 ± 5.02^{A}				
4 °C	0.38 ± 0.04	0.04 ± 0.01	9.9 ± 0.4^{A}	0.12 ± 0.03	0.02 ± 0.00^{A}	5.8 ± 0.3^{A}	1.32 ± 0.23^{A}	59.23 ± 7.55^{A}	595 ± 258	1539 ± 299^{A}	-7.9 ± 2.1^{A}	28.1 ± 0.4^{A}
15 °C	0.47 ± 0.03	0.05 ± 0.00	10.2 ± 0.1^{AB}	0.13 ± 0.01	0.03 ± 0.00^{B}	3.9 ± 0.1^{BC}	10.12 ± 2.26^{B}	81.27 ± 8.99^{AB}	357 ± 320	837 ± 656^{A}	-6.6 ± 3.8^{AB}	28.1 ± 0.5^{A}
25 °C	0.43 ± 0.05	0.04 ± 0.01	10.1 ± 0.2^{AB}	0.11 ± 0.00	0.02 ± 0.00^{AB}	4.7 ± 0.5^{B}	0.08 ± 0.07^{A}	100.69 ± 13.97^{B}	181 ± 105	1283 ± 630^{A}	-7.1 ± 1.1^{A}	31.3 ± 0.6^{B}
35 °C	0.47 ± 0.09	0.04 ± 0.01	10.6 ± 0.2^{B}	0.12 ± 0.02	0.03 ± 0.01^{B}	3.7 ± 0.3^{C}	19.86 ± 1.39^{C}	59.89 ± 7.82^{A}	991 ± 505	33363 ± 14455^{B}	-0.8 ± 0.5^{B}	35.2 ± 1.2^{C}

Table 1: Soil chemical variables and bacterial growth parameters. Growth rates were measured at eight temperatures between 4 to 40 °C. We show here changes in bacterial growth rates in response to the incubation temperature at a high (35 °C) and a low temperature (4 °C) to represent the range of measurement temperatures. Different letters indicate a significant ($P < 0.05$) difference between temperatures as assessed by one-way analysis of variance (ANOVA) followed by Tukey HSD post hoc test. TC = total carbon, TN = total nitrogen, DOC = dissolved organic carbon, DON = dissolved organic nitrogen, T_{opt} = optimum temperature for bacterial growth, T_{min} = minimum temperature for bacterial growth, growth 4 = bacterial growth rates at 4 °C, growth 35 = bacterial growth rates at 35 °C, T0 = time 0 (pre-experiment control)

	eggNOG		CAZy		NCycDB		16S and 18S rRNA genes	
	F	P	F	P	F	P	F	P
Full dataset	10.344,10	< 0.0001***	6.973,8	0.0003***	7.244,10	< 0.0001***	11.464,10	< 0.0001***
Without 35 °C	1.933,8	0.0002***	1.892,6	0.0043**	1.703,8	0.0002***	6.173,8	0.0003***
Without 25 and 35 °C	2.812,6	0.0036**	2.941,4	0.1	1.922,6	0.0032**	18.352,6	0.0043**

Table 2: Temperature effects on functional gene structures assessed with eggNOG via md5nr, CAZy, NcycDB as well as on microbial community structures were assessed using permutational multivariate analysis of variance (PERMANOVA). The analyses were conducted in the full dataset and with subsequent removal of the highest temperature to test if also lower temperatures led to significant difference in functional gene and community structures. Subscripted indices indicate the numerator and residual degrees of freedom for the F-value. * $P < 0.05$; ** $P < 0.01$; *** $P < 0.001$

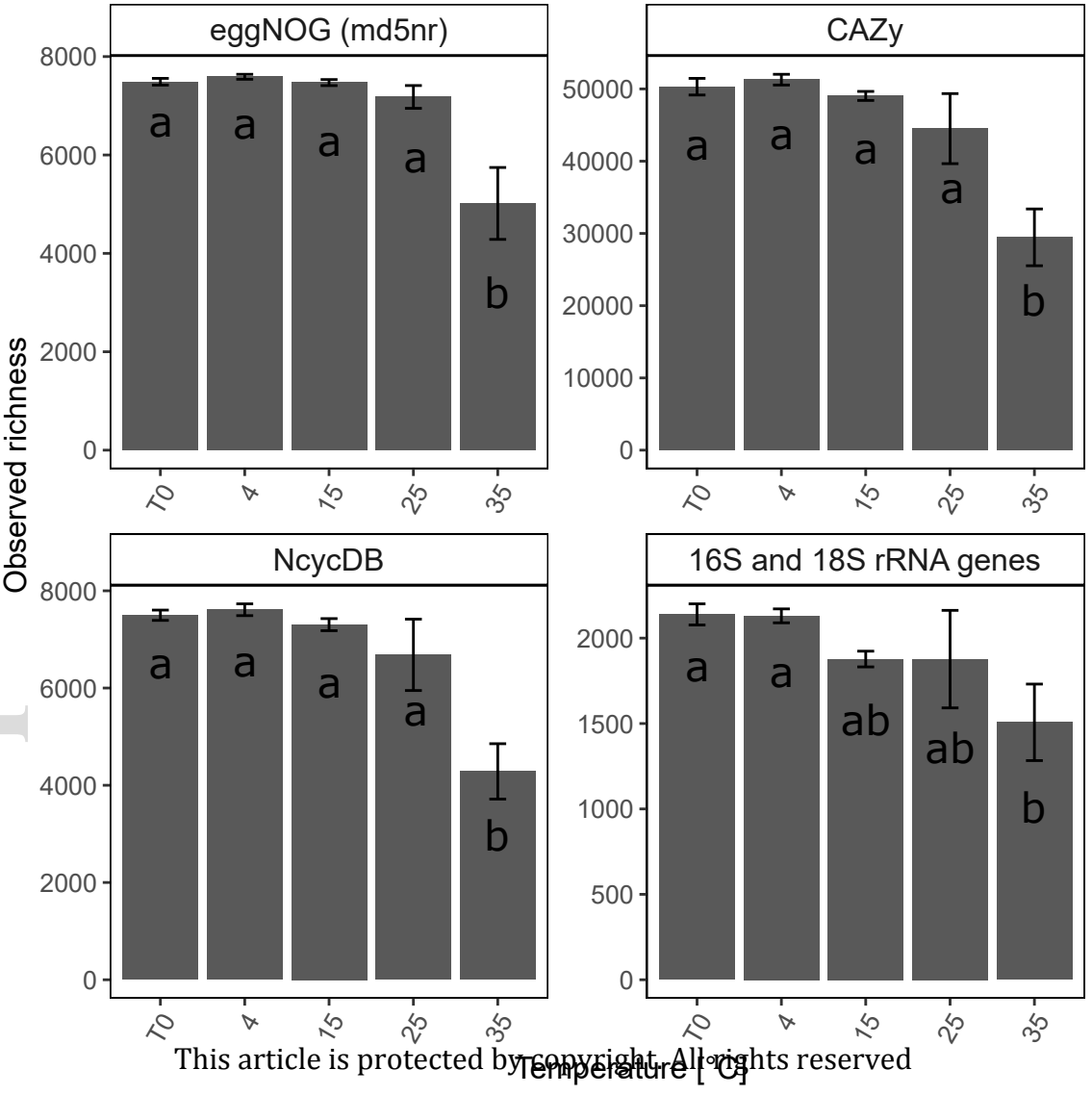

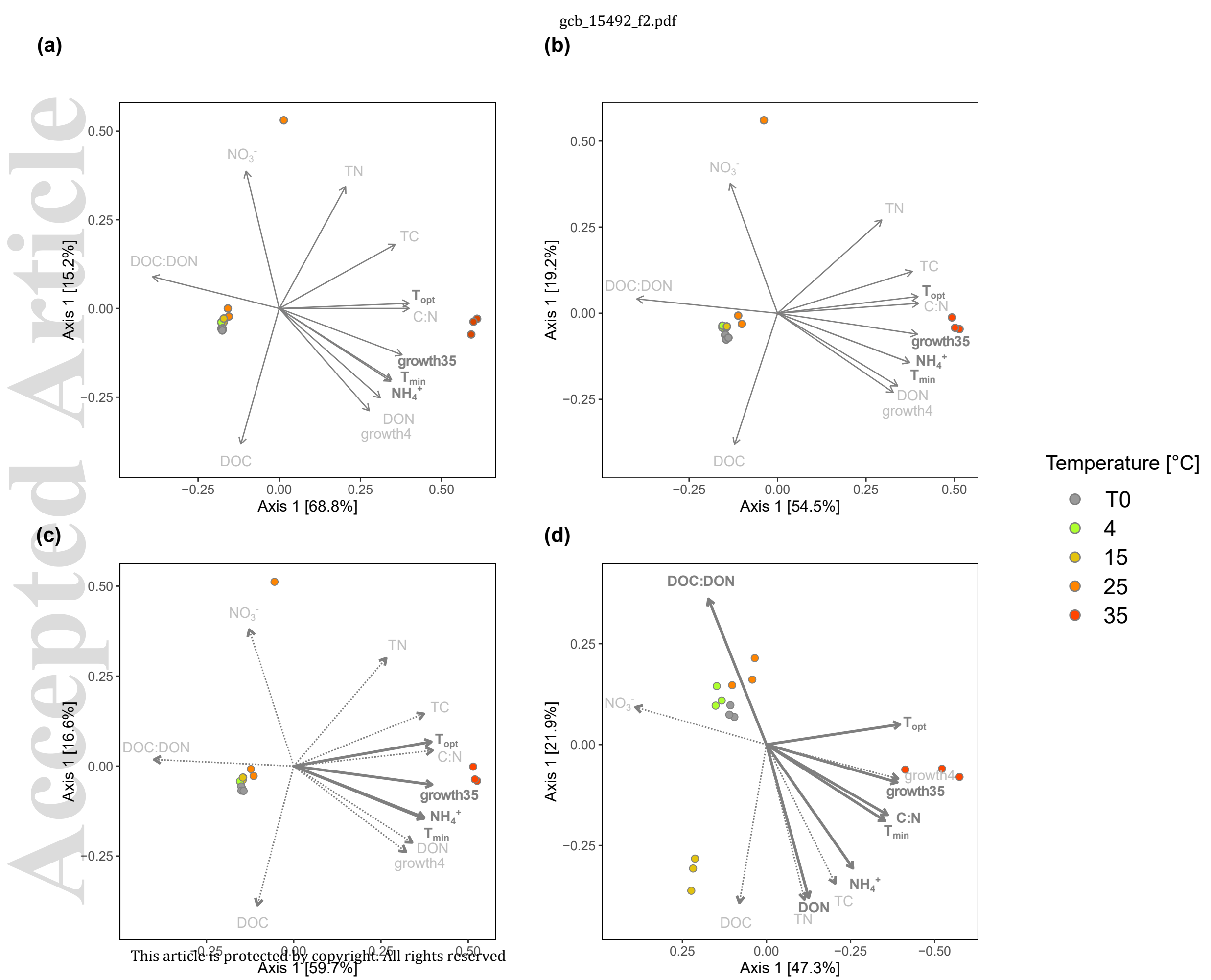

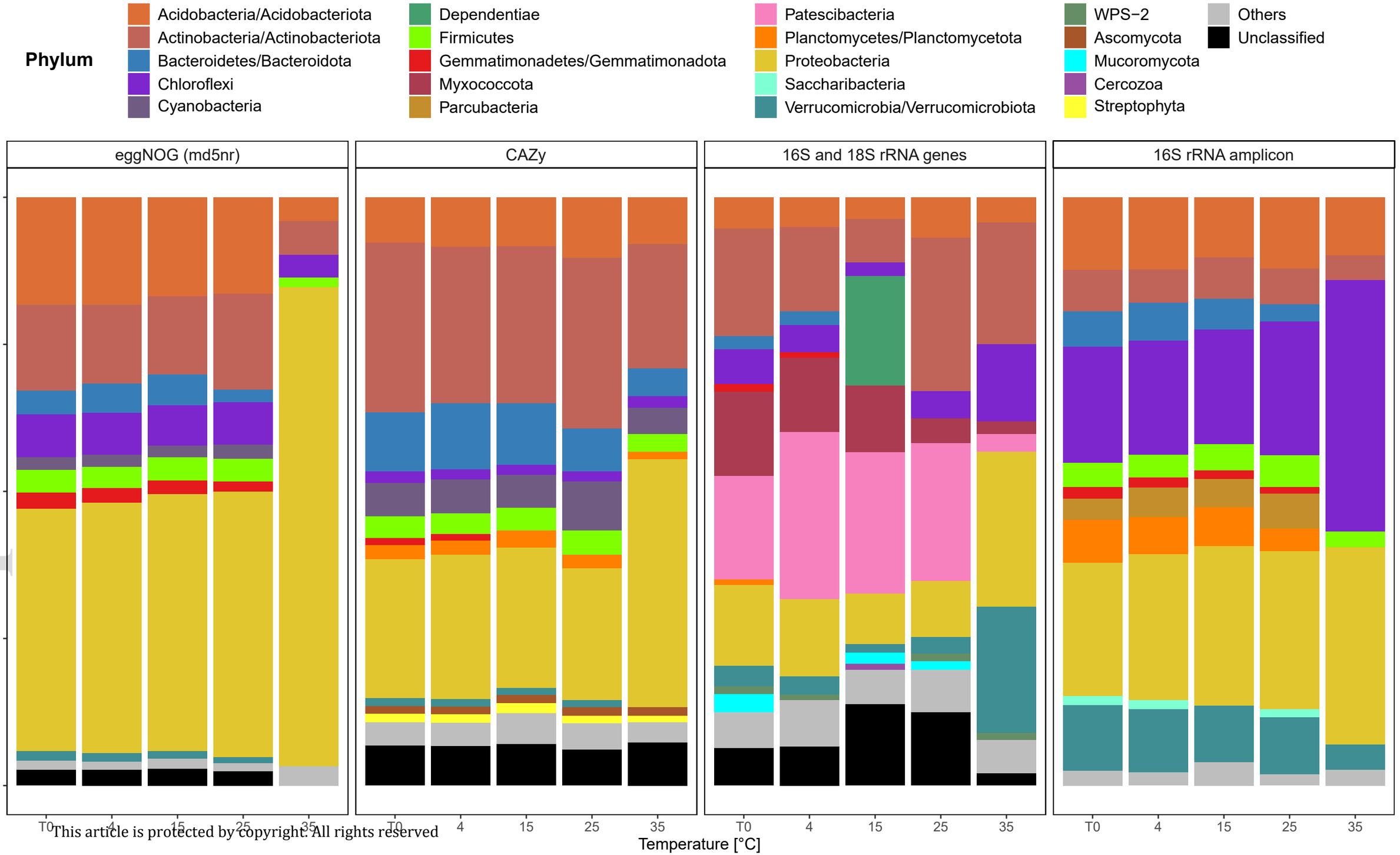

gcb_15492_f4.pdf

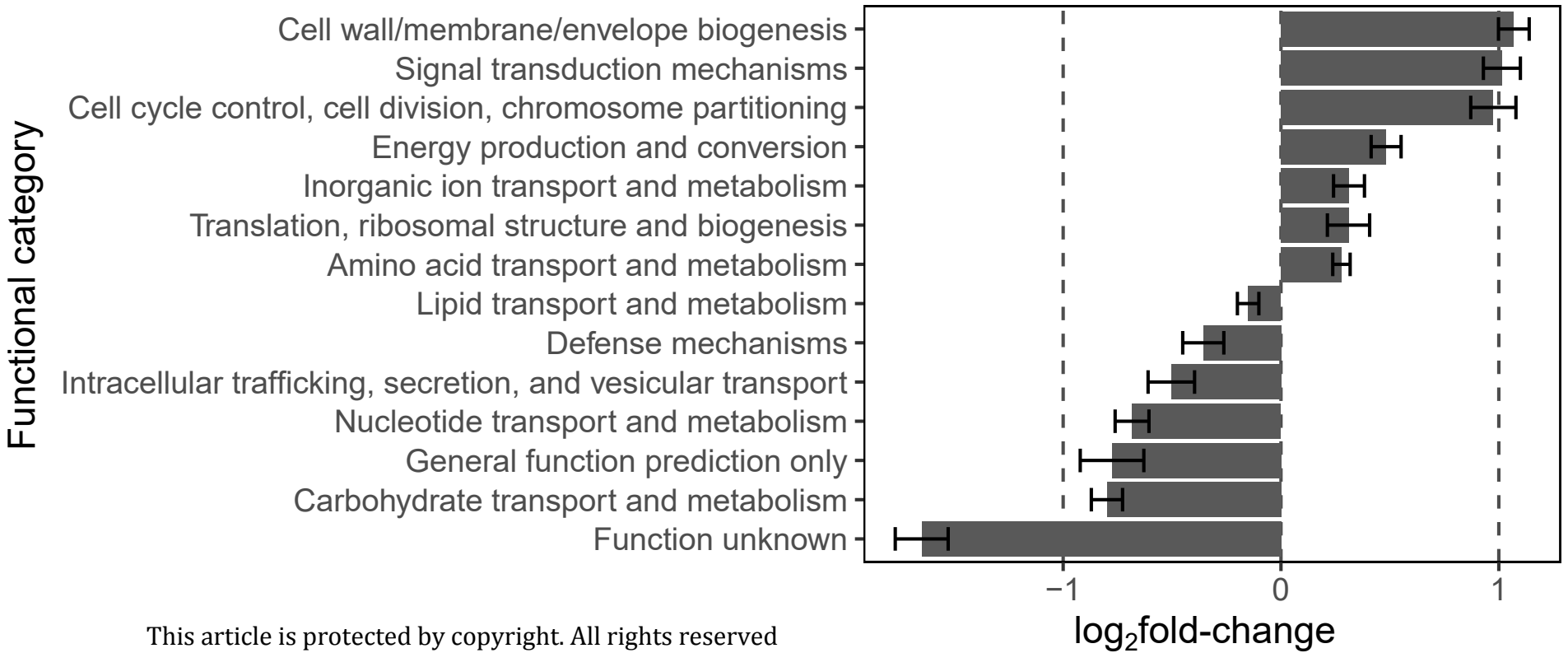

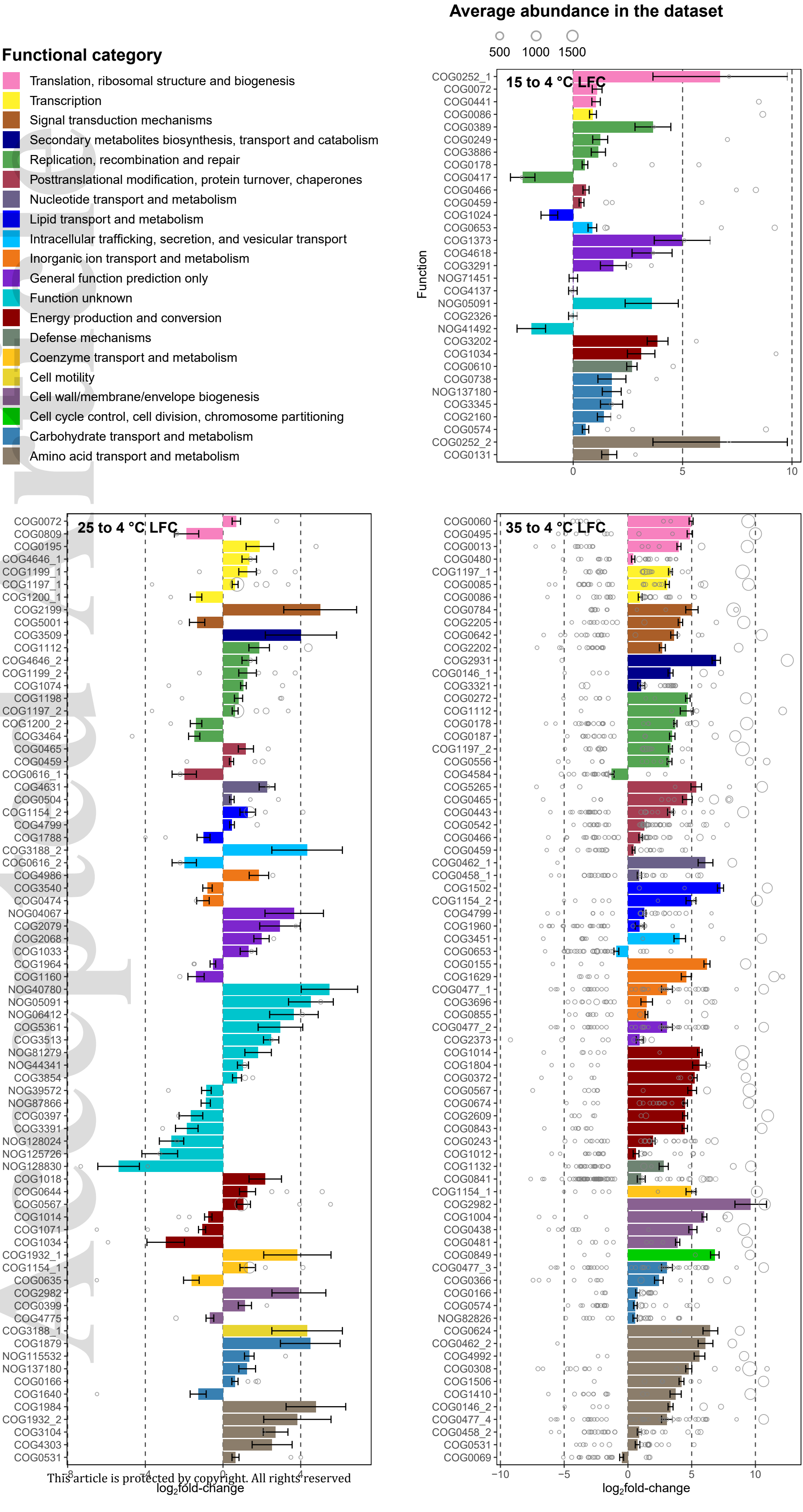

Average abundance in the dataset

- 500
- 1000
- 1500

gcb_15492_f7.pdf

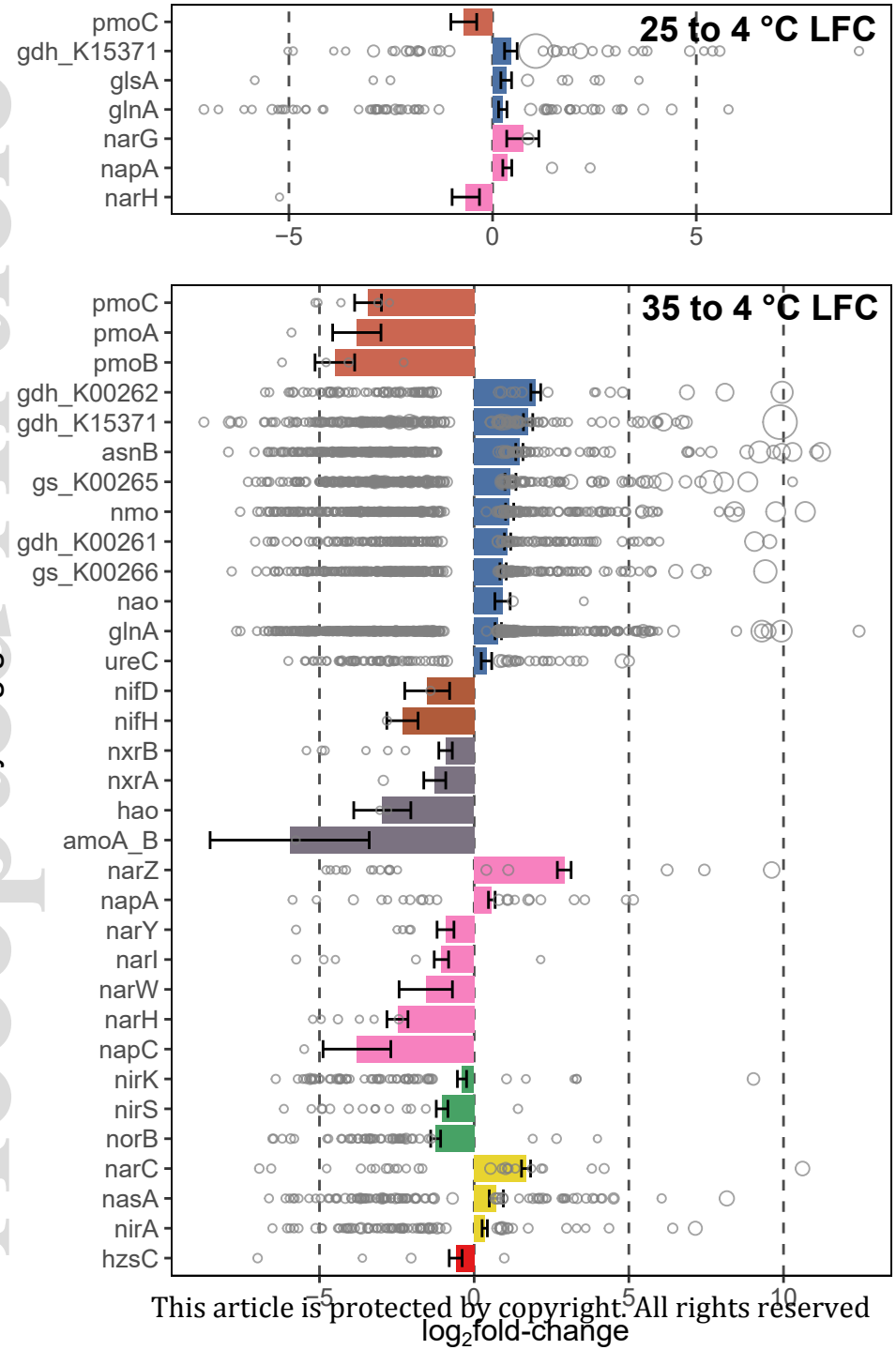

Average abundance in the dataset

- 1000
- 2000
- 3000

N-cycling process

- Others
- Organic degradation and synthesis
- Nitrogen fixation
- Nitrification
- Denitrification; Dissimilatory nitrate reduction
- Denitrification
- Assimilatory nitrate reduction
- Anammox